

University of Mississippi

eGrove

Electronic Theses and Dissertations

Graduate School

1-1-2021

SOLUBILITY MEASUREMENTS OF HYDROPHOBIC SOLUTES IN SUPERCRITICAL CARBON DIOXIDE AND SUBSEQUENT IMPREGNATION INTO PAPER SUBSTRATES FOR SURFACE MODIFICATIONS

Arghavan Beheshtimaal
University of Mississippi

Follow this and additional works at: <https://egrove.olemiss.edu/etd>

 Part of the [Chemical Engineering Commons](#)

Recommended Citation

Beheshtimaal, Arghavan, "SOLUBILITY MEASUREMENTS OF HYDROPHOBIC SOLUTES IN SUPERCRITICAL CARBON DIOXIDE AND SUBSEQUENT IMPREGNATION INTO PAPER SUBSTRATES FOR SURFACE MODIFICATIONS" (2021). *Electronic Theses and Dissertations*. 2087.
<https://egrove.olemiss.edu/etd/2087>

This Thesis is brought to you for free and open access by the Graduate School at eGrove. It has been accepted for inclusion in Electronic Theses and Dissertations by an authorized administrator of eGrove. For more information, please contact egrove@olemiss.edu.

SOLUBILITY MEASUREMENTS OF HYDROPHOBIC SOLUTES IN SUPERCRITICAL
CARBON DIOXIDE AND SUBSEQUENT IMPREGNATION INTO PAPER SUBSTRATES
FOR SURFACE MODIFICATIONS

A Thesis

Presented for the degree of Master of Science

in Engineering Science

Chemical Engineering Department

The University of Mississippi

Arghavan Beheshtimaal

August 2021

Copyright © 2021 by Arghavan Beheshtimaal

ALL RIGHTS RESERVED

ABSTRACT

Supercritical Fluids (SCFs) have received a great deal of attention for their various applications in chemical, biochemical, pharmaceutical, and materials processing. In this study, we investigate surface modification to paper substrates using supercritical impregnation (SCI) techniques, with applications in food packaging. One of the key factors required for this study is understanding the solubility of hydrophobic solutes in supercritical carbon dioxide (scCO₂). Polar compounds are poorly soluble in scCO₂ due to their lack of polarity and frequently co-solvents are also introduced to enhance solubility. In this study, the maximum solubility of alkyl ketene dimer (AKD)/n-heptane and vegetable wax (VW)/n-heptane solutions have been measured by “Cloud Point” methods, with heptane introduced to enhance the solubility of the AKD and VW in scCO₂. Different temperatures (40, 50, 60 °C) and pressures (101.35-172.02 bar) were investigated to identify solubility conditions for subsequent paper impregnation processes, where the presence of AKD improves the hydrophobicity of the paper.

Collected data demonstrates at lower temperatures, higher pressure is needed to dissolve specific amounts of wax/n-heptane solution in scCO₂. Therefore, one can expect the highest solubility of the sample occurs at T = 60 °C. However, at certain temperatures and pressures, retrogradation phenomena may be observed, where the opposite becomes true, and higher solubility occurs at lower temperatures. This was experimentally observed with AKD/n-heptane solubility studies at T=40 and 50 °C conditions. Paper samples were impregnated with AKD/n-heptane at pre-determined solubility conditions and their hydrophobicity was subsequently

measured by a contact angle goniometer. For example, at a temperature of $T = 60\text{ }^{\circ}\text{C}$ and 125.83 bar, the maximum solubility of AKD/n-heptane was 0.1875 mL, and the average of contact angle was 130.75° (this value was taken on day 14 after impregnation). However, at $40\text{ }^{\circ}\text{C}$, the maximum solubility of AKD/n-heptane was 0.1275 mL, and the resulting CA after 14 days was only 106.70° .

Applying annealing treatment typically did not improve the CA significantly compared with the non-annealed values, although at $T = 60\text{ }^{\circ}\text{C}$ and 148.10 bar with $160\text{ }^{\circ}\text{C}$ annealing temperature, the CA was much improved at earlier times compared with non-annealed samples. SEM images showed that the sample impregnated at $T = 40\text{ }^{\circ}\text{C}$ and without annealing is more uniform but at $T = 50\text{ }^{\circ}\text{C}$, better micro-roughness was achieved after annealing (4h, $160\text{ }^{\circ}\text{C}$).

Design of experiment (DOE) with Design-Expert software, a powerful tool for numerical optimization, was used to analyze the collected solubility data. Results' confirmation validates the solubility measurements for all temperatures with the cloud point method to do the experiments and furthermore proves the authenticity of the cloud point measurements with the pressure cell.

DEDICATION

I dedicate my thesis to my parents and my best friends. A special feeling of gratitude to my loving parents, Manizheh Saraeimoghadam and Majid Beheshtimaal, whose words of encouragement and push for tenancy ring in my ears.

ACKNOWLEDGEMENT

I want to express my deepest appreciation to my committee chair and advisor Dr. Brenda Prager who continuously supported and guided me throughout my study at The University of Mississippi.

TABLE OF CONTENTS

ABSTRACT.....	ii
DEDICATION.....	iv
ACKNOWLEDGEMENT.....	v
LIST OF TABLES.....	x
LIST OF FIGURES.....	xii
CHAPTER I.....	1
INTRODUCTION.....	1
CHAPTER II.....	3
BACKGROUND AND LITERATURE REVIEW.....	3
2.1 Functional Barrier Food Packaging and its Environmental Impact.....	3
2.2 Hydrophobic Waxes for Packaging.....	4
2.3 Quantifying Hydrophobicity.....	6
2.3.1 Experimental Considerations.....	6
2.3.2 The Sessile Drop Method.....	7
2.3.3 Factors Affecting Hydrophobicity of a Surface and Development of Superhydrophobicity.....	8
2.4 SCFs and Their Applications.....	10

2.4.1 Characteristics of Supercritical Fluids.....	11
2.4.2 Use of Co-solvents with SCF	13
2.5 Prediction of Solute Solubility in SCF.....	15
2.6 Experimental Determination of Solute Solubility in SCF Using Cloud Point Methods.....	16
2.7 Purpose of this Work.....	17
CHAPTER III	19
MATERIALS AND METHODS.....	19
3.1 Material	19
3.2 High-pressure Cell Cleaning Method.....	19
3.3 Solubility measurements	21
3.4 Density Measurements for Wax/n-heptane with Pycnometer.....	22
3.5 Paper Impregnation Process with AKD	23
3.6 Mass of Hydrophobic Solute impregnated into the Paper.....	23
3.7 CA Measurements	23
CHAPTER IV	25
RESULTS AND DISCUSSION.....	25
4.1 Experimental Results.....	25

4.1.1 Solubility Measurements of AKD/n-heptane in scCO ₂ with “Cloud Point Experiment”	25
4.1.2 Solubility Measurements of VW/n-heptane in scCO ₂ with “Cloud Point Experiment”	30
4.1.3 Correlations between SCI at Cloud-Point Solubility Conditions for AKD/n-heptane/scCO ₂ , and Hydrophobic Development of Treated Paper	33
4.1.4 Effects of Impregnation and Annealing on the Paper Surface	44
4.2 Design Results	53
4.2.1 Design of Experiment (DOE)	53
4.2.2 Design Objectives and Factors Affecting the Experimental Design	54
4.2.3 Factors for Cloud Point Experiment Designs	54
4.2.3 AKD/n-heptane Cloud Point Pressure Design	55
4.2.4 VW/n-heptane Cloud Point Pressure Design	62
CHAPTER V	69
CONCLUSION AND RECOMMENDATIONS	69
5.1 Conclusion	69
5.2 Recommendations	71
LIST OF REFERENCES	73

LIST OF APENDIX	79
APENDIX A	80
Cloud Point Images for wax/n-heptane.....	80
VITAE.....	84

LIST OF TABLES

Table 2.1. Properties of selected fluids	13
Table 4.1. Quantities of AKD/n-heptane dissolved in scCO ₂ at T=40, 50 and 60 °C and various pressures.....	26
Table 4.2. Quantities for VW/n-heptane dissolved in scCO ₂ at T=40, 50 and 60 °C and various pressures.....	31
Table 4.3. Conditions to impregnate the paper substrate with AKD/n-heptane solution and the subsequent annealing temperatures.....	34
Table 4.4. AKD mass impregnated into the paper substrates and CO ₂ density at different conditions.....	42
Table 4.5. Impregnation process conditions for preparing the paper substrates in scCO ₂ . Also shown is the measured CA at day 14 for these conditions (assumed approximately constant from Day 14 onwards), and short descriptions of the samples based on SEM observations.....	44
Table 4.6. Multilevel Categorical Design factors and levels for AKD/n-heptane.....	55
Table 4.7. Multilevel Categorical Design factors and response value for AKD/n-heptane.....	55
Table 4.8. Quantities of AKD/n-heptane dissolved in scCO ₂ at T=40, 50 and 60 °C	56
Table 4.9. ANOVA table from design-expert for AKD/n-heptane.....	58
Table. 4.10. Multilevel Categorical Design factors and levels for VW/n-heptane.....	62

Table. 4.11. Multilevel Categorical Design number of runs, factors and the response value for VW/n-heptane.....63

Table 4.12. Quantities of VW/n-heptane dissolved in scCO₂ and cloud point pressures for design.....63

Table 4.13. ANOVA table from design-expert for VW/n-heptane in scCO₂.....64

LIST OF FIGURES

Figure 2.1. Chemical structure of AKD. R1 and R2 represent straight carbon chains of lengths varying between 16 and 18 atoms.....	5
Figure 2.2. Red angle shows the CA on the surface.....	8
Figure 2.3. Cassie-Baxter State: Air is trapped underneath the liquid drop.....	9
Figure 2.4. Phase behavior of ethanol/1-butyl-3-methylimidazolium acetate ([Bmim]Ac)/scCO ₂ at 40 °C. (a) 0 MPa, two phases: LV; (b) 13.56 MPa, cloud point.....	17
Figure 3.1. Diagram of supercritical rig for paper impregnation process with scCO ₂ . The blue lines show how the pressure-cell is connected to the system.....	20
Figure 3.2. Image of the high-pressure cell for measuring the solubility of wax/n-heptane in scCO ₂	21
Figure 3.3. Image of pycnometer for measuring wax/n-heptane density.....	22
Figure 4.1. Mole fraction of AKD/n-heptane dissolved in scCO ₂ at T=40, 50 and 60 °C. Mass quantities of AKD were converted to moles using an average molecular weight of 504 (g/mol)...	27
Figure 4.2. Cloud point observed at T=51 °C and P=172.02 bar. Additional images are in Appendix A (p. 80).....	27
Figure 4.3. Relationship between ln Solubility and ln CO ₂ density for AKD/n-heptane solution in scCO ₂	28

Figure 4.4 Mole fraction of VW/n-heptane dissolved in scCO₂ at T=40, 50 and 60 °C. Mass quantities of VW were converted to moles using an average molecular weight of 720 g/mol provided by KOSTER KEUNEN.....31

Figure 4.5. Relationship between ln Solubility and ln CO₂ density for VW/n-heptane solution in scCO₂.....32

Figure 4.6. Mean CA VS days for the impregnated paper with AKD/n-heptane in scCO₂ at T=40 °C and two different pressures without annealing temperature.....35

Figure 4.7. Mean CA VS days for the impregnated paper with AKD/n-heptane in scCO₂ at T=50 °C and two different pressures without annealing temperature.....35

Figure 4.8. Mean CA VS Days for the impregnated paper with AKD/n-heptane in scCO₂ at T=60 °C and two different pressures without annealing temperature.....35

Figure 4.9. Mean CA measurements versus time for AKD-paper impregnated at T=40 °C and two different pressures with three annealing temperatures. (a) impregnated sample at a lower pressure and (b) impregnated sample at a higher pressure.....37

Figure 4.10. Mean CA measurements versus time for AKD-paper impregnated at T=50 °C and two different pressures with three annealing temperatures. (a) impregnated sample at a lower pressure and (b) impregnated sample at a higher pressure.....39

Figure 4.11. Mean CA measurements versus time for AKD-paper impregnated at $T=60\text{ }^{\circ}\text{C}$ and two different pressures with three annealing temperatures. (a) impregnated sample at a lower pressure and (b) impregnated sample at a higher pressure.....40

Figure 4.12. Actual AKD/n-heptane mass impregnated into the paper versus pure CO_2 density...43

Figure 4.13. Figure 4.13. SEM micrographs of (a) plain paper and (b) AKD-impregnated paper with (an excess amount of AKD/n-heptane solution), impregnated at room temperature and $P=200$ bar, after 10 days. SEM images (c-f), AKD-impregnated papers (1.8 g/L, $T = 40\text{ }^{\circ}\text{C}$, $P=155.82$ bar), before and after annealing (4 h, $160\text{ }^{\circ}\text{C}$). Images (g-j) AKD-impregnated papers (1.8 g/L, $T = 50\text{ }^{\circ}\text{C}$, $P=156.10$ bar), before and after annealing (4 h, $160\text{ }^{\circ}\text{C}$). low magnifications (c-d, g-h) and high magnifications (e-f, i-j) show the morphology and structure of the paper substrates for $T = 40$ and $50\text{ }^{\circ}\text{C}$50

Figure 4.14. Half-Normal Plot from Design-Expert for AKD/n-heptane solution in scCO_257

Figure 4.15. Normal plot of residual and residual versus predicted obtained from design-expert for AKD/n-heptane in scCO_258

Figure 4.16. Interaction graph extracted from design-expert, for AKD/n-heptane cloud point pressure (MPa) versus temperature ($^{\circ}\text{C}$).....59

Figure 4.17. Interaction effect extracted from design-expert, for AKD/n-heptane cloud point pressure (MPa) vs solution (mL).....60

Figure 4.18. 3D surface plot from design-expert for AKD/n-heptane cloud point pressure (MPa) VS temperature and amount of AKD/n-heptane (mL).....	61
Figure 4.19. Half-Normal Plot from Design-Expert for VW/n-heptane solution in scCO ₂	64
Figure 4.20. Normal plot of residual and residual versus predicted obtained from design-expert for VW/n-heptane in scCO ₂	65
Figure 4.21. Interaction effect extracted from design-expert, for VW/n-heptane cloud point pressure (MPa) vs solution (mL).....	66
Figure 4.22. 3D surface plot from design-expert for VW/n-heptane cloud point pressure (MPa) VS temperature and amount of VW/n-heptane (mL).....	67
Figure A.1 Cloud point observed at T=40 °C and P=165.47 bar.....	78
Figure A.2 Cloud point observed at T=50 °C and P=110.32 bar.....	78
Figure A.3 Cloud point observed at T=60.3 °C and P=106.87 bar.....	79
Figure A.4 Cloud point observed at T=57.4 °C and P=161.89 bar.....	79
Figure A.5 Cloud point observed at T=40.3 °C and P=106.87 bar.....	80
Figure A.6 Cloud point observed at T=41.7 °C and P=166.03 bar.....	80
Figure A.7 Cloud point observed at T=49.7 °C and P=146.86 bar.....	81

CHAPTER I

INTRODUCTION

The food industries are one of the largest consumers of packaging. Different plastics such as polypropylene, polyethylene terephthalate, and polyvinyl chloride are widely applied due to their low weight, low cost, and availability. The consumption of these materials damages the environment drastically [1]. Thus, using biodegradable and eco-friendly materials which are obtained from renewable sources such as papers for food packaging applications is a good solution [2, 3]. Since the paper has a hydrophilic nature, it can easily absorb moisture from the environment which harms the quality of food [3] and reduces its worth as a package.

To improve hydrophobicity, paper is usually coated with various biodegradable components such as food-grade waxes to provide hydrophobicity to the paper at a low price [3]. Food-grade waxes such as vegetable wax (VW) and alkyl ketene dimer (AKD) create excellent hydrophobicity and result in a barrier against moisture to protect food from the environment. One approach to make the paper more hydrophobic is to apply supercritical impregnation (SCI) of waxes into paper for substrate improvements as an easy and simple process with minimal harm to the environment. In this impregnation process, the supercritical fluid (SCF) is supercritical carbon dioxide (scCO₂) and the wax solute is first dissolved into this fluid under appropriate conditions before penetrating the paper substrate to make it more hydrophobic [4].

The purpose of this study is to determine the solubility of wax/n-heptane solutions in scCO₂ at different pressures and temperatures using cloud point methods and then use these conditions to supercritically impregnate the waxes into paper substrates for improved hydrophobicity. The resulting paper substrates impregnated with wax/n-heptane solution will have improved barrier against moisture and will represent an environmentally friendly method for preparing food packaging materials.

1.1 Research Objectives

Various research objectives have been pursued to achieve the overall goal:

- 1- To measure the maximum solubilities of AKD/n-heptane and VW/n-heptane in scCO₂ at different pressures and temperatures of 40, 50, and 60 °C using cloud point experimental methods. These maximum solubilities of wax/n-heptane in scCO₂ are proportional to the amount that can be impregnated into substrate fibers and matrixes during the impregnation process.
- 2- To impregnate the paper substrate with AKD/n-heptane in scCO₂ using solubility conditions, and perform contact angle (CA) measurements on the resulting substrates to correlate impregnation conditions with paper hydrophobicity.
- 3- To explore the effects of annealing the impregnated samples on hydrophobic development, and investigate changes in roughness and porosity of the resulting treated papers.
- 4- To apply the design of experiment (DOE) with design-expert software to identify the cloud point pressures' trends for AKD and VW at temperatures of 40, 50, and 60 °C by “Multilevel Categorical Design”, and undertake statistical analyses of this data using ANOVA methods.

CHAPTER II

BACKGROUND AND LITERATURE REVIEW

2.1 Functional Barrier Food Packaging and its Environmental Impact

One of the largest industries that consumes considerable amounts of packaging is food industries all over the world. Several plastics such as polyethylene, polystyrene, polypropylene, and polyvinyl chloride are largely applied [1] in producing packaging due to their convenience, durability, low- cost [5], and great physiochemical properties. The big problem in using polymer-based packaging is harming the environment since these materials are not biodegradable and their recycling rate is low. One possible approach to enhance the properties of the bio-based polymers is to use hydrophobic materials such as oils or waxes in producing bi-layer films to reduce water vapor permeability (WVP) which is an essential parameter in food packaging materials. For example, carnauba wax as a non-expensive wax increases the opacity and decreases water vapor permeability and solubility which is favorable for food packaging materials. Also, the effect of cold plasma treatment with carnauba wax coating will result in a strongly hydrophobic outer surface of the protein film which is desirable for food packaging materials [1].

The sources of pollution on earth are a global issue and prove the importance of applying renewable sources for food coating and packaging [3]. One way of minimizing the negative environmental impacts is to utilize paper and paperboard materials for food packaging applications due to their biodegradable and mechanical properties. However, these materials possess properties such as high porosity and permeability to some gases and also to moisture which is not suitable

for packaging food products. To resolve this issue, hydrophobic synthetic materials such as polyethylene coat paper layers to enhance water barrier properties are a possible solution. For instance, coating a paper with wheat gluten helps in improving its barrier properties against water vapor and gases. Another example is mandarin waste which can improve the water and gas barriers of Kraft paper. Results of air transmission rate and water vapor properties demonstrated boosted stability against oxidative reactions of Kraft paper. Substances extracted from citrus waste are appropriate for food packaging to protect foods from oxygen deterioration and to extend their shelf-life. Furthermore, the hydrophilic nature due to the presence of OH-groups should be improved by a coating process as well [3].

Papers are usually coated with a variety of polyolefin materials and during this process paper loses its biodegradable potentials, making recycling difficult. Therefore, to ensure sustainable development, providing hydrophobicity with natural hydrophobic compounds such as carnauba wax and chitosan have been studied [3].

2.2 Hydrophobic Waxes for Packaging

AKD has been used as a sizing agent for a long time in the paper industry. AKD wax with a melting point of 40 - 60 °C acts by increasing the Contact Angle (CA) of the fiber to levels of around 110 °. This fact will create capillary resistance against moisture penetration for the paper surface [6]. Moreover, combining the behavior of AKD with other compounds such as dialkyl ketone (DAK) can produce superhydrophobicity for other types of substrates as well. The chemical structure of AKD is shown in Figure 2.1 [6].

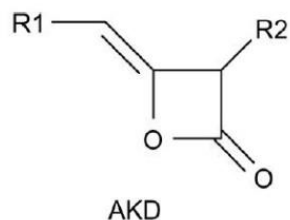


Figure 2.1. Chemical structure of AKD. R1 and R2 represent straight carbon chains of lengths varying between 16 and 18 atoms [6].

Vegetable wax (VW) as a food-grade wax is obtained by full or partial hydrogenation of vegetable oils (VO) such as palm oils or soybean. Usually, this hydrophobic wax needs more chemical modifications to achieve favorable functionalities to enhance useful physical properties and also to compete with optimized petroleum-based waxes. VW has a melting point of 44 - 54 °C and can penetrate paper substrates via SCI to improve their hydrophobicity and mechanical strength [4, 7].

Other waxes used to enhance hydrophobicity include plant epicuticular waxes, which are complex mixtures existing on the outer surface of plants. They are also used as food-grade materials to create barriers against abiotic loss of water, fungi, and also UV radiation. Results of a study by Jyoti Yadav et. al [3] demonstrated that the highest hydrophobicity on paper discs was achieved by using benzene to extract the wax.

2.3 Quantifying Hydrophobicity

Hydrophobicity is an essential property for a packaging substrate surface in contact with water and is determined both by its geometrical structure of the surface and its chemical nature [6]. Cellulose paper substrates show high polarity due to the existence of OH-groups in their structures which have a high affinity with water to create hydrogen bonds. Thus, to develop hydrophobicity for a cellulose paper a lowering of the surface energy and raising of the substrate surface roughness is needed. As stated earlier AKD, a waxy substance derived from fatty acids has been utilized in the paper industry as a sizing agent to improve the hydrophobicity of the paper [8]. The most common method to assess the degree of hydrophobicity of a surface is contact angle (CA) measurements utilizing the Young–Laplace method [6].

2.3.1 Experimental Considerations

Preparation of the specimens, maintaining the cleanliness of the instrument and sample, and the isolation of the instrument from external effects such as vibration and changes in temperature are important precautions to take before and during CA measurements. Other factors such as smoothness, and the stability of the targeted surface both chemically and dimensionally can affect the results of CA measurements. Thus, all imperfections related to the substrate can affect the recorded data for CAs [9].

In general, CA measurements are performed at room temperature and in the open atmosphere of the laboratory. Placing the sample directly on the instrument stage is acceptable for some hydrophobic substrates, but lack of equilibration between the phases in an open system may be an important matter. Placing the sample inside a glass cell covered with a polymeric film

(Parafilm) or a metallic foil through which a needle may be inserted is a good approach for doing CA measurements [9].

Isolating the sample from the lab environment has two important advantages [9]:

- 1- The covered glass cell protects the sample from dust and any other organic contamination that can deposit on the surface of the sample during or before the CA measurements.
- 2- When the solid sample is inside the glass cell, the cell is saturated with liquid vapors.

In addition, to the aforementioned precautions, the syringe and needle should be cleaned and dried before the CA measurement. A good practice is to clean inside the syringe and needle with DI water (water that has had all of the ions removed) before and after filling it with water or other organic liquids for each experiment [9].

2.3.2 The Sessile Drop Method

In the context of the present study, CA is the angle a liquid droplet makes between its surface in contact with air and its surface in contact with a solid plane. Figure 2.2 shows the CA of one drop on the solid surface. The vertex of this CA occurs at the intersection of the three phases: air, liquid, and solid. The sessile drop method is applied by a contact angle analyzer instrument which operates by image analysis of the drop profiles to determine the CA using the Young-Laplace equation [9]. Measuring the contact angle by depositing the liquid drop on the surface is a common way to investigate the wettability of a material's surface. Wetting is the phenomenon that shows how a liquid deposited on a solid (or liquid) substrate spreads out, and the ability of liquids droplets to form boundaries with substrate surfaces. If the tendency for wetting is larger, the contact angle is smaller, and true wetting is defined when the CA is 0° [10].

Contact angle measurement is a useful surface characterization method that provides information on hydrophobicity and morphology of the surface which is affected by many factors such as surface roughness, surface preparation methods, the temperature of the surrounding environment, and the cleanliness of the surface when taking CA measurements [10].

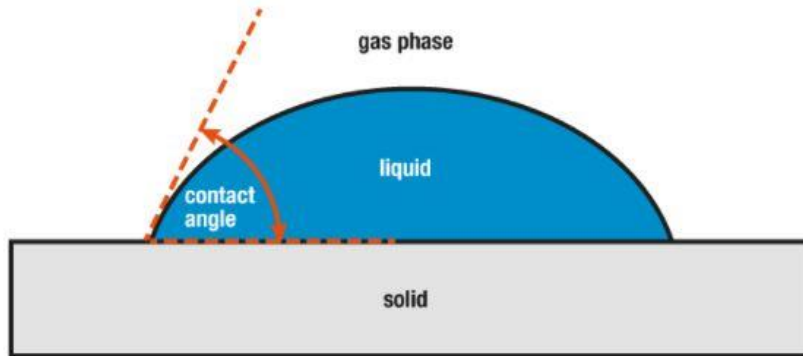


Figure 2.2. The red angle shows the CA on the surface.

2.3.3 Factors Affecting Hydrophobicity of a Surface and Development of Superhydrophobicity

The CA of the drop that deposits on the surface of the substrate provides significant information about the surface roughness which improves hydrophobicity. Superhydrophobic surfaces such as plant leaves are good examples of self-cleaning substrates from water drops that are almost spherical and can easily roll off these surfaces, removing dust particles and other contaminants. Typically, this is called the lotus effect which relates to superhydrophobic surfaces. It is known from the experiments with Lotus leaves a Cassie drop (drop that sits on the roughness peaks) rolls easily on the surface of the substrate and shows less hysteresis. Therefore, it is essential to create superhydrophobic rough surfaces such that a Cassie drop is formed [11].

2.3.3.1 Cassie Baxter Equation

The Cassie Baxter equation describes the effective contact angle for a liquid on chemically heterogeneous surfaces, originally derived from an equation for smooth solid surfaces [8]:

$$\cos\theta = r\cos\theta - f(r\cos\theta_0 + 1) \quad (2.1)$$

f is the fraction of air-liquid interface, θ is the measured CA on the porous surface, θ_0 is the intrinsic CA on smooth surface and r is the rough surface area divided by flat projected area. When air pockets are present on a rough single-component surface, the Cassie-Baxter equation can also be used for the contact angle estimation of a water drop on this surface as seen schematically in Figure 2.3 [8]. Moreover, the Cassie-Baxter equation was found to be useful in the analysis of chemically heterogeneous flat surfaces as well as air pockets containing rough surfaces [8].

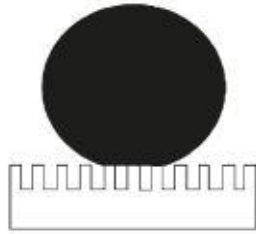


Figure 2.3. Cassie-Baxter State: Air is trapped underneath the liquid drop.

2.3.3.2 Surface Roughness

The behavior of the droplet of a liquid that sits and rolls on a surface is determined by both the surface chemistry and the surface roughness. A flat hydrophobic surface that exhibits a contact angle of 115° can be enhanced to a superhydrophobic surface showing a contact angle of greater than 150° by roughening the surface of the substrate [12].

Considering superhydrophobic surfaces, one way of changing the roughness of the substrate is to apply a coating to the substrate surface, creating a superhydrophobic surface with

different contact angle hysteresis (CAH) [12]. The important reason behind the superhydrophobic surface is that most of the areas occupied by air are due to the porosity of the substrate surface, and only a small fraction of the surface supporting the water droplet is covered with hydrophobic materials such as paraffin and polytetrafluoroethylene (PTFE) [13].

In recent years there has been significant interest in developing water-repellent surfaces [11]. Such surfaces show high potential in various applications from anti-sticking, anti-contamination, and self-cleaning to coatings and anti-corrosion [11, 12]. In parallel, many studies have shown that more complete knowledge is required to understand the influence of evaporation on CAs and water drop shape for a better understanding of numerous dynamic wetting processes on different surfaces. Since CAs change when the inevitable vaporization of a water drop in air occurs, this knowledge is essential in characterizing surface properties [12].

2.4 SCFs and Their Applications

SCI of waxes such as AKD into the paper substrate are simple processes and have minimal damage to the environment. For these impregnation processes, the SCF is $scCO_2$ and the solute is first dissolved into this fluid at appropriate solubility conditions. The solute dissolves in the $scCO_2$ and passes through the substrate and, due to its gas-like diffusivity, completely penetrates the porous matrix and coats the fiber surface. It is assumed that the high-pressure impregnation technique distributes the solute throughout the substrate uniformly [4] and eventually, all surface areas of the substrate have been modified from this SCI process. Additionally, the surface roughness and hydrophobic improvement of the wax develop slowly with time, as in the case of AKD [8].

2.4.1 Characteristics of Supercritical Fluids

Gaseous compounds are defined as supercritical fluids with isothermal compressibility much higher than liquid [14] when their pressure and temperature exceed their critical pressure and temperature respectively. Depending on their thermodynamic properties, supercritical fluids behave either like a liquid or a gas [15, 16, 17]. Several industries use supercritical technology as a benign environmental technology. Application of supercritical fluids are now either at commercial scales in many areas or still under more investigation [18]. One important fact about the supercritical region is its transformation from a liquid-like density to vapor-like density by adjusting the temperature or pressure [15,16]. In addition, near the critical region, small changes in temperature or pressure result in large changes in density [15, 16, 19]. For several years most of the attention has been on inexpensive, nonexplosive, low viscosity, easily removable, and environmentally friendly carbon dioxide, as it is a readily available supercritical fluid [15, 16, 17, 20].

To have a better understanding of supercritical fluids, the following facts should be considered [21]:

- 1- In supercritical fluids, the solvent strength is a function of density which changes with pressure and temperature. Thus, pressure, temperature, and density are of prime importance in processes dealing with supercritical fluids and by using a modest change in temperature and pressure all density-dependent parameters such as solubility parameter, or dielectric constant may vary markedly [14, 21].
- 2- One of the main applications of SCFs is in the extraction industry, as SCFs have faster extraction than those with liquid solvents.

- 3- SCFs show significantly lower viscosity than liquids, which is a desirable flow property.
- 4- scCO_2 is easily removed from the targeted substance via depressurization, which is very desirable and significant in industrial processes.
- 5- Finally, SCF should be nontoxic, available in high purity, and inexpensive.

In addition to the above considerations, critical pressure and temperature are the most important characteristics in choosing the appropriate supercritical fluid. The properties of some of the selected fluids which could apply in supercritical fluid extraction (SFE) have been provided in Table 2.1 [21].

Table 2.1. Properties of selected fluids [21].

Fluid	Critical Temperature ($^{\circ}$ C)	Critical Pressure		
		bar	atm	psi
Carbon Dioxide	31.1	73.8	74.8	1070.4
Ethane	32.42	48.8	49.5	707.8
Methanol	40.10	80.90	82.0	1173.4
Ammonia	132.4	113.5	115	1646.3
Nitrous Oxide	36.61	72.4	73.4	1050.1
Xenon	16.7	58.4	59.2	847.0
Water	374.4	221.2	224.1	3208.2
Chlorodifluoromethane	96.3	49.7	50.3	720.8

For many applications of SCF such as extractions, impregnation processes, and reactions, a high diffusion coefficient is essential which leads to a higher rate of mass transport [22]. For instance, in impregnation processes, a homogenous distribution of an active compound within porous matrixes is achieved by the diffusivity of supercritical fluids, laden with solutes such as aromas in food products, preservatives in wood, and many more [18].

2.4.2 Use of Co-solvents with SCF

SCF applications are not restricted to the aforementioned areas and can be applied to a variety of fields such as environmental remediation, removal of toxic contaminants from soil, cracking reactions of coal for liquefaction, polymer processing, nanotechnology, enhanced oil recovery technology, and many others [20, 22]. However not being able to dissolve hydrophilic molecules or materials with high molecular weight such as colloids, proteins, and many other polymers restrict its applications [20].

Since solubility is a property of a substance in a particular solvent [23], selecting an appropriate cosolvent to improve the solubility of the desired solute is essential in supercritical processes [19, 24]. In many studies, SCF is mixed with a cosolvent to provide higher solubility in that specific medium [20, 22]. Fluid mixtures containing organic cosolvent are expected to have a higher solubility in the SCF than without the cosolvent. In general, a small amount of cosolvent which is a polar, or a non-polar organic compound miscible in SCF, truly acts as a modifier that can change the polarity and strength of the primary SCF which leads to higher solubilities of desired solutes [22].

Examinations show there is a hydrogen bonding and charge transfer complex formation between solute and cosolvent. The addition of cosolvent in the system can affect physical interactions in a solution such as dipole-dipole, dipole-induced dipole, or induced dipole-induced dipole interactions between solute and cosolvent [25]. Since solubility increases exponentially with density, and the density of SCF can be altered with pressure and temperature, the addition of cosolvent in the solution has a significant effect on the solubilities of solutes in SCFs [25]. Furthermore, SCFs density and transport properties such as viscosity, and other physical properties like polarity, change drastically with a small variation in pressure and temperature near the critical point. Therefore, it is possible to tune a unique combination of properties necessary for the desired application to obtain solubility enhancement [26].

In general, two frequently used cosolvents are acetone and alcohol. These choices allow the study of many different effects such as hydrogen bonding in SCFs. Experimental data revealed that the cosolvent effect for some combination of the solute and cosolvent increases with pressure, especially when there is a strong interaction such as 2-naphthol with cosolvent ethanol or acetone [25]. This may happen due to the proximity to an upper critical end point (UCEP) region where

small variations in temperature or pressure can have large effects on solubility. Another key fact is a decrease in the solvent effect resulting from increased pressure. This happens because the critical pressure of carbon dioxide is larger than the critical pressure of cosolvents such as ethanol, acetone, and isopropanol [25]. Although the effect of nonpolar organic compound cosolvents such as n-hexane in scCO₂ on solubility is limited, the solubility of ionic liquids dramatically increases in scCO₂ with polar organic compounds such as acetone [27].

2.5 Prediction of Solute Solubility in SCF

Most of the methods applied in solubility prediction for solutes in SCF are based on correlations between solubility and solute molecular structure. Since the application of statistical mechanical models, solution thermodynamic approaches, and equation of state methods are limited, the most practical approach has been introduced by King and Friedrich (1990). King and Friedrich introduced the solubility parameter theory which relates to the understanding of solute behavior in dense gases and it consists of four basic factors [21]:

- 1- **Miscibility Pressure**: At this pressure, the solute begins to dissolve in the fluid. Also, this concept was introduced as a threshold pressure that may change according to the method used to monitor the solute concentration in the SCF.
- 2- **Maximum solubility pressure**: This pressure is that which the highest amount of solute has been dissolved in the supercritical fluid and at this point, the solubility parameter of the solute equals that of the fluid.
- 3- **Fractionation pressure range**: This concept describes the pressure range between the miscibility pressure and the maximum solubility pressure in which the solute's solubility varies from zero to its possible maximum solubility.

- 4- **Solute physical properties:** A significant parameter is the solute's melting point and most solutes have increased solubility in a SCF when in liquid form. Moreover, temperature changes will affect solubility parameters [21].

In addition to the above factors, some other parameters such as particle size, temperature, and molecular weight of the solute affect solubility in different ways [26]:

- 1- **Particle size:** As a particle becomes smaller the surface area to volume ratio increases, and a greater interaction occurs at the larger surface area.
- 2- **Temperature:** If the solution process absorbs energy, the solubility increases with an increase in temperature, but if the process releases energy, the solubility will decrease when increasing the temperature. For example, in gases, solute solubility decreases as the temperature of the solution increases.
- 3- **Molecular Size:** The solubility of the solute is decreased when it has a higher molecular weight and larger molecular size is more difficult to surround the solute with solvent molecules to solvate the compound [26].

2.6 Experimental Determination of Solute Solubility in SCF Using Cloud Point Methods

The cloud point is a key measurement that enables maximum solubility determination of a given solute within a supercritical fluid. These types of measurements can experimentally confirm predicted solubilities from thermodynamics modeling [28, 29]. Solubility of ILs in scCO₂ obtained much attention due to their high chemical and thermal stability [28, 29], and are described here to demonstrate experimental cloud point methods. To observe a cloud point in a typical experiment, a specific amount of the IL and cosolvent is put inside the pressure view cell (reactor). When the temperature reaches the desired value, CO₂ is compressed into the reactor, the pressure

is increased, and it is tuned by controlling the high-pressure syringe pump until a single phase is achieved and finally, the cloud point is obtained by adjusting the volume plunger. Figure 2.4 [28] shows the development of this cloud point. At the bottom of the cell, there is a magnetic stirrer.

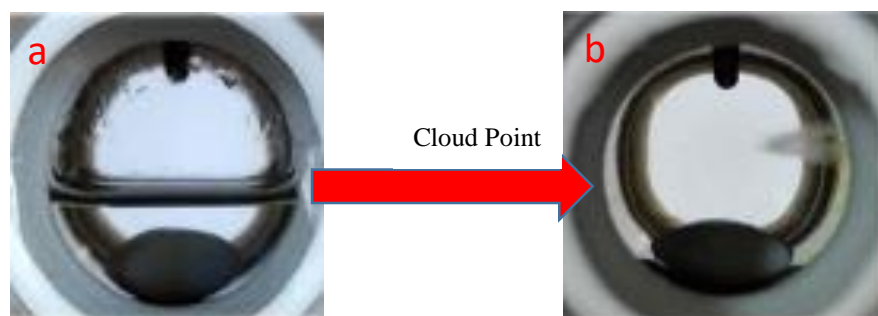


Figure 2.4. Phase behavior of ethanol/1-butyl-3-methylimidazolium acetate ([Bmim]Ac)/scCO₂ at 40 °C. (a) 0 MPa, two phases: LV; (b) 13.56 MPa, cloud point [28].

The presence of ethanol cosolvent with higher concentration in the system forms stronger interactions, dissolves more IL in scCO₂, and eventually, the density of the cosolvent/scCO₂ mixture increases with increasing concentration [28].

Considering different temperatures, the solubility of [Bmim]-AC did not increase for all scCO₂/cosolvent mixture systems. For instance, using ethanol as the cosolvent the solubility of [Bmim]-Ac increased in scCO₂. On the other hand, the solubility of [Bmim]-AC decreased by using acetone as a cosolvent instead of ethanol in scCO₂. Therefore, the effect of temperature on solubility varies depending on the cosolvent used in the system [28].

2.7 Purpose of this Work

Knowing the fact that AKD and VW are food-friendly materials for the food packaging industry creates interest in applying SCI methods with these waxes to improve the hydrophobicity of paper substrates. The main purpose of this work is to determine the maximum solubility of

wax/n-heptane in scCO₂ and use these solubility conditions to supercritically impregnate these waxes into paper substrates to make them more hydrophobic. Correlations between maximum solubility limits as determined via solubility studies, and actual quantities of impregnated waxes into the paper will be investigated. Furthermore, the effects of annealing treatment on the modified paper with respect to hydrophobicity will be studied via CA measurements and SEM imaging for various impregnated samples with AKD/n-heptane to identify the optimum solubility pressure and temperature that results in the most hydrophobic paper substrate. Finally, cloud point pressure trends will be predicted for wax/n-heptane in scCO₂ by “Multilevel Categorical Design” using Design-Expert software and then statistically analyzed using ANOVA methods. Design graphs for the predicted cloud point pressures of AKD/n-heptane and VW/n-heptane hydrophobic solutions in scCO₂ will also be presented.

CHAPTER III

MATERIALS AND METHODS

3.1 Material

AKD wax with an average molecular weight of 504 (g/mol) (Aquapel™ 364 K sizing agent) containing chain lengths of C16 to C18 was supplied by Solenis. VW with an average molecular weight of 720 (g/mol) was provided by KOSTER KEUNEN, and n-heptane 99.5 % were bought from Sigma Aldrich. Wax/n-heptane solutions were prepared at concentrations of 1.8 g/L and 10 g/L of AKD and VW solutions, respectively. Supercritical fluid-grade carbon dioxide was provided by Airgas USA, LLC. Deionized (DI) water was mechanically filtered using a Direct-Q 3UV system to remove impurities through an electrically charged resin to make it suitable for use.

3.2 High-pressure Cell Cleaning Method

Cleaning was critical in collecting reliable data for cloud point experiments, and the high-pressure cell was cleaned in two stages.

In the first stage, a hand pump (High-Pressure Equipment) was filled with DI water before connecting it to a 5 mL THAR high-pressure view cell (Water Corporation). The DI water was passed through the cell three times, followed by three flushes with ethanol. During this cleaning procedure, the exit valve of the view cell remained open to remove the excess solvents. The cell was subsequently opened and wiped with Kimwipes to remove any remaining DI water or ethanol.

In the second stage, the pressure cell was disconnected from the hand pump and then connected to the syringe pump (Teledyne ISCO). The syringe pump was filled to 240-260 mL with CO₂ and pressurized 20-40 psi higher than the pressure of the CO₂ tank. By running the syringe pump, CO₂ gas was pressurized inside the cylinder up to the set point shown on the screen. When the pressure reached the set value the first and the second pressure-valves (Figure. 3.1) connected to the view cell were opened respectively to pressurize the cell. At this stage, the Valve (V1') connected to the view cell was opened to let CO₂ gas flush through the view cell for few seconds. This part was repeated three times and for the final cleaning by CO₂ the view cell was heated up a few degrees higher than CO₂ critical temperature to complete the cleaning procedure. Finally, all remaining solvents and contaminants were cleaned with Kimwipes. Figure 3.2 shows the image of the actual high-pressure solubility measurements.

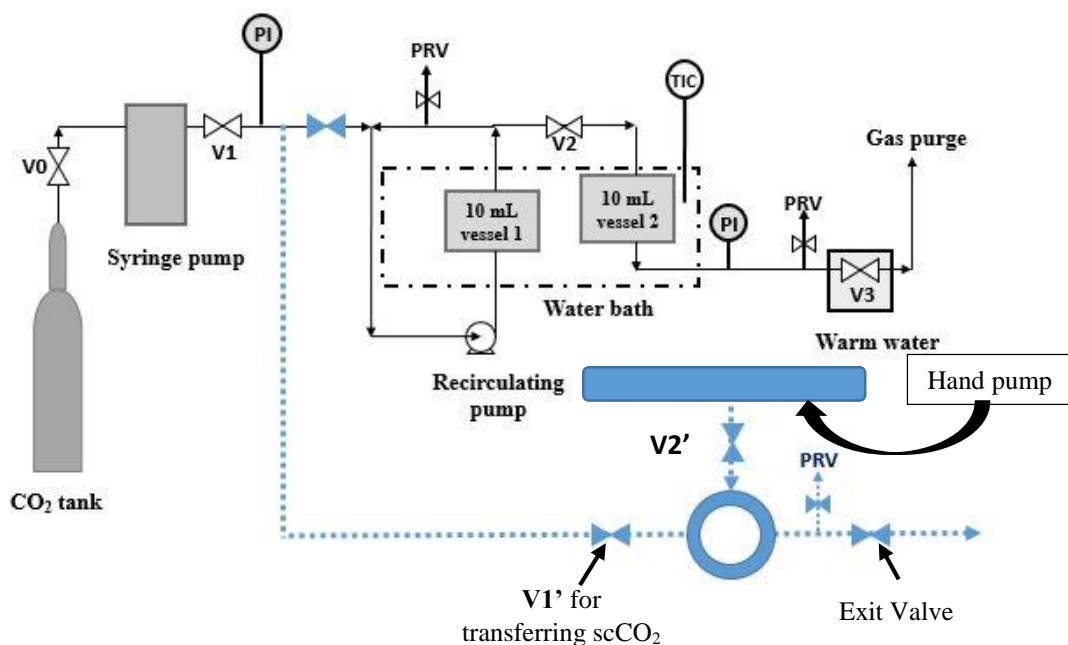


Figure 3.1. Diagram of the supercritical rig for paper impregnation process with scCO₂. The blue lines show how the pressure-cell is connected to the system.

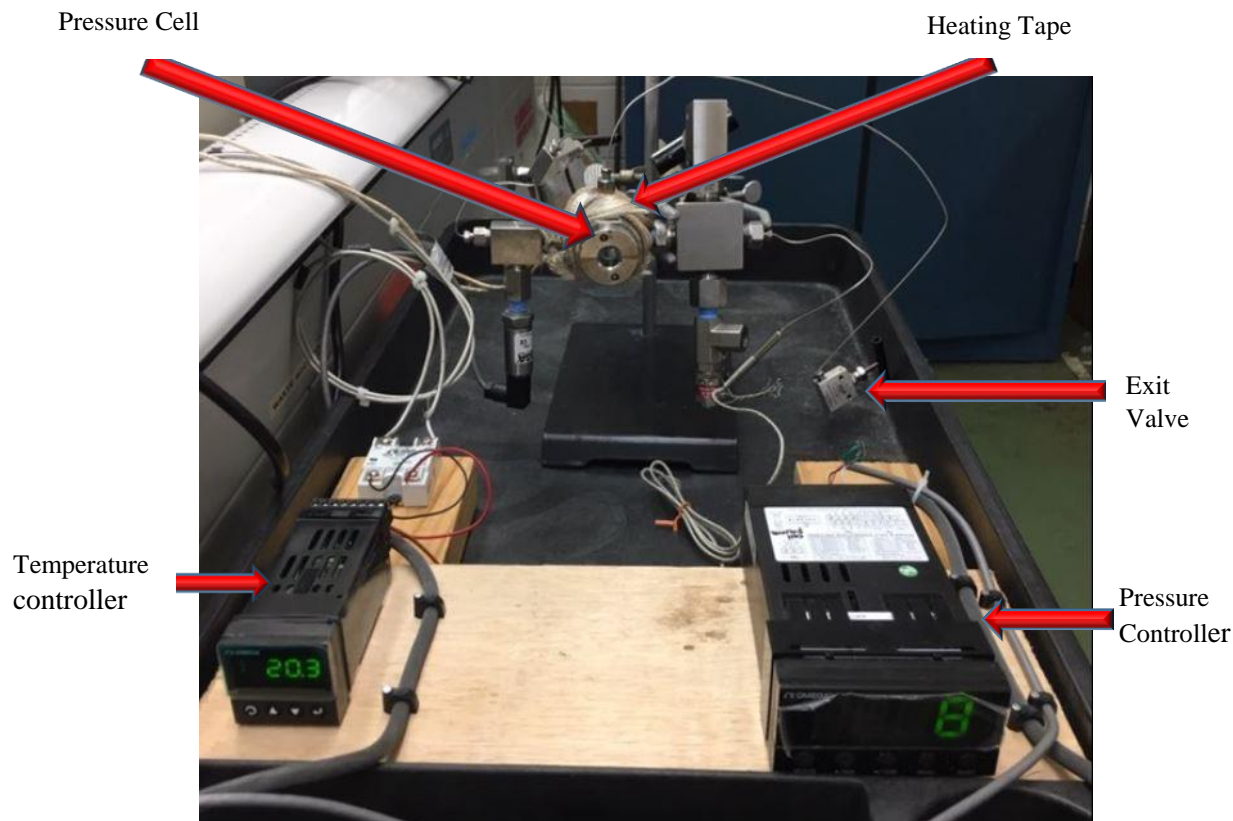


Figure 3.2. Image of the high-pressure cell for measuring the solubility of wax/n-heptane in scCO₂.

3.3 Solubility measurements

The solubility measurements were conducted by filling the hand pump (Figure 3.2) with a wax/n-Heptane solution and then connecting the cell to the hand pump for pressurization. Consequently, the hand pump was pressurized by turning the handle to the right 360 degrees to deliver a pre-determined quantity of wax/n-Heptane solution to the view cell. The pressure valve before the cell was opened slowly and the number of wax/n-Heptane solution drops that entered the view cell was counted. The volume of wax/n-heptane sample was determined by multiplying the number of the sample drops by the volume of each drop which was measured as 0.00994 ± 0.0016 for AKD/n-heptane and 0.0130 ± 0.0011 for VW/n-heptane (the mass of several drops of these solutions were measured; converted to volume using corresponding solution density and

finally divided by the number of the drops for individual drop volume). At this point, the cell was disconnected from the hand pump and reconnected to the filled syringe pump. The syringe pump was set and run to a pressure near the expected onset of the cloud point behavior. The first and second exit valves were opened respectively to transfer the scCO₂ into the view cell, and the pressure and temperature were subsequently recorded. Typically, the cloud point measurements were determined by increasing the pressure from the original set point by 180-250 psi until the sample was dissolved completely in scCO₂. The entire experiment was completed by transferring specific amounts of wax/n-heptane sample into the view cell and then pressurizing it up to a certain value for T = 40, 50, and 60 °C.

3.4 Density Measurements for Wax/n-heptane with Pycnometer

The mass of the Pycnometer (KIMAX) before and after filling with wax/n-heptane solutions was measured. Using the density formula (density=mass/volume), the mass of each sample (1.8 g/L AKD/n-heptane and 10 g/L VW/n-heptane) was divided by the volume of the Pycnometer which was 25 mL, and the density of both waxes was obtained. The density of AKD/n-heptane is 0.6845 (g/cm³) and the density of VW/n-heptane is 1.2044 (g/cm³), taken at room temperature 20 °C. An image of the pycnometer is shown in Figure 3.3.



Figure 3.3. Image of pycnometer for measuring wax/n-heptane density.

3.5 Paper Impregnation Process with AKD

Paper substrates were modified by impregnating them with AKD/n-heptane solution dissolved in scCO₂. In this process (Figure 3.1), two strips of paper were placed inside a 10 mL vessel (V-2) and the hydrophobic AKD/n-heptane solution was injected into vessel 1 (V-1). The syringe pump was filled with CO₂ up to 150 -160 mL, and then pressurized to the desired pressure of the experiment. Valve (V1) was opened and the recirculating pump turned on. The AKD/n-heptane solution was dissolved in scCO₂ for ten minutes, and then the recirculating pump was shut off. The second valve (V2) was opened to impregnate the supercritical solution into the papers for fifteen minutes. Upon completion, the syringe pump was stopped and the last valve (V3) was opened to release the remaining CO₂ inside the system to the fume hood.

3.6 Mass of Hydrophobic Solute impregnated into the Paper

It is important to determine the exact amount of the Wax/n-heptane solution impregnated into the paper substrates. To determine this information, paper strips were weighed before and after the impregnation process. The difference in these masses resulted in the exact mass of the wax/n-heptane solution impregnated into the paper substrate. As the majority of the n-heptane is considered to have evaporated due to its high volatility, the mass value measured was essentially the amount of wax impregnated into the paper substrate.

3.7 CA Measurements

CA measurements were performed on wax-impregnated substrates to investigate surface modifications to the substrate. A Biolin OneAttension Contact Analyzer was used, together with a DI water-filled syringe. Of the four methods available on the computer screen, the “Sessile Drop” method was used for measuring contact angles. The first step was to calibrate the system with the

calibration ball by putting it on the stage, and monitoring the ball's image, then by clicking the calibration button on the screen and seeing the message that the "calibration was successful", the calibration is completed. For successful calibration, the image of the ball needs to cover most of the computer screen, and the needle should be placed exactly on the top of the ball. Next, a small piece of the impregnated paper substrate was cut and placed on the system stage and monitored on the computer screen. The information recorded for each measurement included the name of the experiment, time (s), and the number of pictures taken by the system. At this point, the measurement is started by clicking "run", and the CA analyzer starts forming the water droplet at the tip of the needle, subsequently depositing it onto the surface of the paper substrate. Data is recorded for the right, left and also the mean contact angles versus time, as well as a baseline.

CHAPTER IV

RESULTS AND DISCUSSION

This chapter and the subsequent discussions have been provided in two parts. The first section is the experimental part which includes solubility measurements, parameters that affect solubility in scCO₂, CA measurements for the modified substrates with and without annealing temperatures, and SEM analysis, while, the second section relates to the predicted results for cloud point pressures with Design-Expert software.

Solubility measurements were performed for two food-grade waxes (AKD and VW). Subsequent studies relating solubilities to hydrophobic development of impregnated papers were demonstrated with AKD only, and it is acknowledged that additional work would need to include a similar study with VW impregnations.

4.1 Experimental Results

4.1.1 Solubility Measurements of AKD/n-heptane in scCO₂ with “Cloud Point Experiment”

To measure the maximum solubility of wax/n-heptane in scCO₂, 0.018 g of AKD was dissolved in 10 mL n-heptane and a pre-determined quantity of this solution was placed inside the high-pressure cell. All solubility data were collected for different supercritical pressures between 101.35 bar and 172.02 bar and temperatures of 40, 50, and 60 °C. When all AKD/n-heptane solution inside the cell was completely dissolved in scCO₂, the cloud point temperature and the pressure were recorded. The solubility values for all three temperatures and different pressures are shown in Table 4.1. For instance, at T=50 °C, for 0.2625 mL of AKD/n-heptane, the cloud point

pressure is 140.52 bar and the recorded temperature is 50.8 °C. Figure 4.1 exhibits the solubility of AKD/n-heptane solution in scCO₂ at different pressures and Figure 4.2 shows the observed cloud points in the laboratory with their pressures and temperatures for the highest amounts of AKD/n-heptane solubility in scCO₂. The remaining cloud point images of other conditions may be found in Appendix A (p. 78). Considering all conditions, the amount of AKD/n-heptane dissolved in scCO₂ is between 0.0375 and 0.3600 mL and, at higher pressures more AKD/n-heptane is dissolved in scCO₂ for all three temperatures.

Table 4.1. Quantities of AKD/n-heptane dissolved in scCO₂ at T=40, 50, and 60 °C and various pressures.

Raw Data for AKD/n-heptane								
T = 40 ± 1°C			T = 50 ± 1°C			T = 60 ± 1°C		
P-(bar)	Vol (mL)	Mol-frac	P-(bar)	Vol (mL)	Mol-frac	P-(bar)	Vol (mL)	Mol-frac
101.4	0.0375	0.0034	110.3	0.0525	0.0060	106.9	0.0525	0.0090
104.0	0.0675	0.0059	117.2	0.090	0.0092	110.3	0.0750	0.0120
132.4	0.1275	0.0109	131.0	0.1538	0.0148	117.2	0.1200	0.0170
149.1	0.1725	0.0130	115.8	0.1538	0.0148	125.83	0.1875	0.0228
155.8	0.2025	0.0151	140.5	0.2625	0.0230	127.55	0.1875	0.0228
165.5	0.2325	0.0171	156.1	0.3000	0.0250	137.89	0.2775	0.0297
-	-	-	172	0.3375	0.0271	158.58	0.2775	0.0297
-	-	-	-	-	-	148.10	0.3150	0.0313
-	-	-	-	-	-	159.27	0.3150	0.0313
-	-	-	-	-	-	161.89	0.3600	0.0334

* 'Vol' is the quantity of AKD/heptane that fully dissolved into scCO₂ at the T and P indicated.

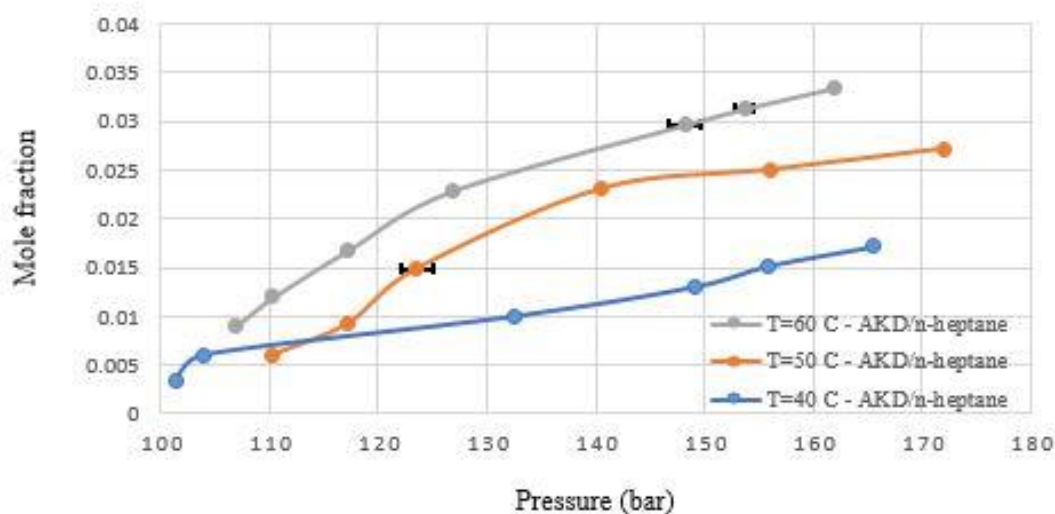


Figure 4.1. Mole fraction of AKD/n-heptane dissolved in scCO₂ at T=40, 50, and 60 °C. Mass quantities of AKD were converted to moles using an average molecular weight of 504 (g/mol).

a) Before pressurization - 0.3375 mL AKD/n-Hep inside the cell.

b) Cloud Point

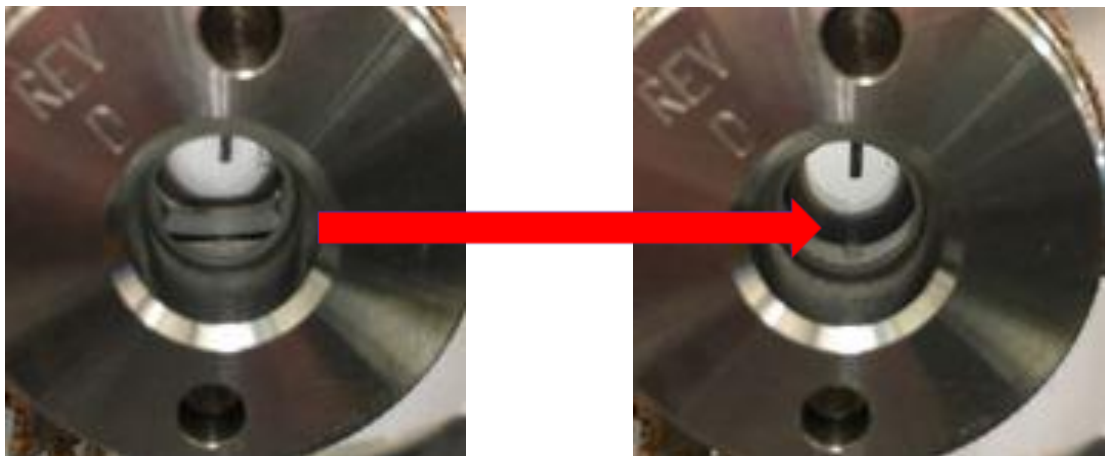


Figure 4.2. Cloud point observed at T=51 °C and P=172.02 bar. Additional images are in Appendix A (p. 78).

Solubilities were determined at three temperatures, 40, 50, and 60 °C, in this work. As illustrated in Figure 4.1, the solubility is increased by increasing the temperature. For example, when the mole fraction of AKD/n-heptane is 0.015 at a pressure of 123.4 bar for T=50 °C, at a lower temperature of 40 °C, 155.8 bar is required to dissolve the same amount of the AKD/n-

heptane in scCO₂. Moreover, by increasing the pressure at all studied temperatures the solubility of the AKD/n-heptane is increased in scCO₂. The reason is that the density of scCO₂ increases with increasing pressure and usually the solubility of the solute increases with increasing scCO₂ density [28]. Solubility results suggest that for the AKD wax as a hydrophobic agent being dissolved in scCO₂ at different conditions, higher pressures provide higher solubilities at a higher temperature.

The existence of retrograde vaporization in solute-SCF systems has been known for some time and has been illustrated in several experimental studies. The crossover pressure is a phenomenological observation that appears to reflect a property characteristic of the solute-solvent system [30, 31]. This is observed in Figure 4.1 at lower pressures, where the temperature increased from 40 °C to 50 °C and the solubility decreased. On the other side of the region the opposite is true and the solubility of AKD/n-heptane solution in scCO₂ increases with an increase in temperature [30].

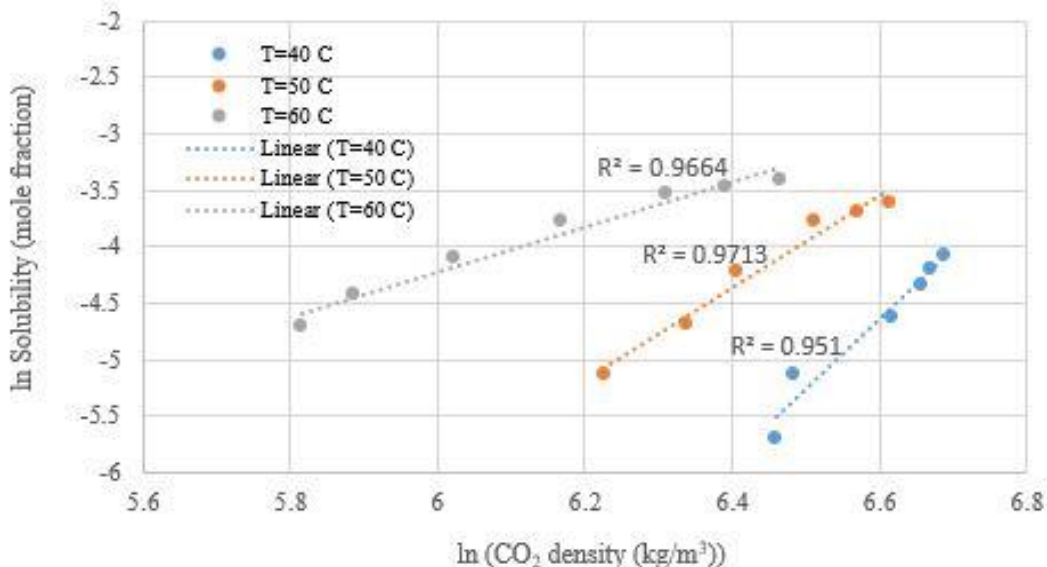


Figure 4.3. Relationship between ln Solubility and ln CO₂ density for AKD/n-heptane solution in scCO₂.

One of the main goals of the solubility measurements with the cloud point experiment is to measure the solubility limit of the AKD/n-heptane solution in scCO₂ at each pressure and temperature. Therefore, understanding the behavior of the hydrophobic solution in scCO₂ can be obtained by plotting the ln (S) which is solute solubility (mole fraction), versus ln (CO₂ density). The trend lines in Figure 4.3 demonstrate the existence of the linear relationship between the ln (S) and ln (CO₂ density), which indicates the fact that the solubility of the AKD/n-heptane increases linearly with increasing the CO₂ density. So, enhanced solubility is possible at higher CO₂ densities. The reliability of the collected data for solubility of the AKD/n-heptane in scCO₂ can be likened to the Chrastil equation which predicts a linear relationship between solute solubility and the density of the solvent, through the following expression [30, 32]:

$$\ln C_2 = k \ln \rho_1 + a / T + b \quad (4.1)$$

Where C_2 is the solubility of the solute, ρ is solvent density, a , b , and k are constants from fitted data, and T is the temperature. Figure 4.3 demonstrated a linear relationship between ln (solubility) and ln (CO₂ density) for measured solubility data by cloud point experiment at all three temperatures, and hence tentatively confirms solubility behavior predicted by the Chrastil equation. The predicted results for ln (solubility) versus ln (CO₂ density) [32] showed the lower temperature lines exist below the higher temperature lines for chlorothalonil (tetrachloroisophthalonitrile), Amical-48 (diiodomethyl *p*-tolyl sulfone), and TCMTB (2-(thiocyanomethylthio) benzothiazole) in scCO₂. This behavior is replicated for the current results.

4.1.2 Solubility Measurements of VW/n-heptane in scCO₂ with “Cloud Point Experiment”

To measure the maximum solubility of VW/n-heptane in scCO₂, 0.10 g of VW was dissolved in 10 mL n-heptane and a pre-determined quantity of this solution was placed inside the high-pressure cell. All collected solubility data for VW/n-heptane in scCO₂ were between 104.88 and 180.64 bar and temperatures of 40, 50, and 60 °C. The cloud point pressure and the temperature were recorded after all VW/n-heptane solutions dissolved in scCO₂. For all three temperatures, the solubility of VW/n-heptane increases with increasing pressure, and one can expect higher solubilities at higher pressures. Considering all recorded data, VW/n-heptane quantities dissolved in scCO₂ are between 0.6500 and 1.1050 mL. As stated earlier 0.10 g of VW dissolved in 10 mL n-heptane, but only 0.018 g of AKD dissolved in the same amount of n-heptane, thus, one can expect higher solubilities for VW/n-heptane in scCO₂ at different temperatures and pressures. Recorded quantities of VW/n-heptane are shown in Table 4.2, and Figure 4.4 shows the mole fraction amounts at the cloud point for each solubility condition. No crossover pressure is observed with these studies, in contrast to the AKD/n-heptane results shown in Figure 4.1.

Table 4.2. Quantities for VW/n-heptane dissolved in scCO₂ at T=40, 50, and 60 °C and various pressures.

Raw data for VW/n-heptane								
T=40±1 °C			T=50±1 °C			T=60±1 °C		
P-(bar)	Vol-(mL)	Mol-frac	P-(bar)	Vol-(mL)	Mol-frac	P-(bar)	Vol-(mL)	Mol-frac
106.86	0.6500	0.1049	104.80	0.6500	0.1505	108.59	0.6500	0.1843
128.93	0.7800	0.1158	111.14	0.6500	0.1326	102.73	0.6500	0.2036
166.03	0.8450	0.1174	118.38	0.7800	0.1447	111.14	0.7800	0.2096
167.96	0.8450	0.1172	123.42	0.7800	0.1383	110.32	0.7800	0.2124
180.64	0.9100	0.1247	127.00	0.8450	0.1463	111.70	0.8450	0.2210
-	-		137.21	0.9750	0.1609	119.28	0.8450	0.2017
-	-		146.86	1.1050	0.1769	138.24	0.9100	0.2113

*Vol is the quantity of VW/heptane that fully dissolved into scCO₂ at the T and P indicated.

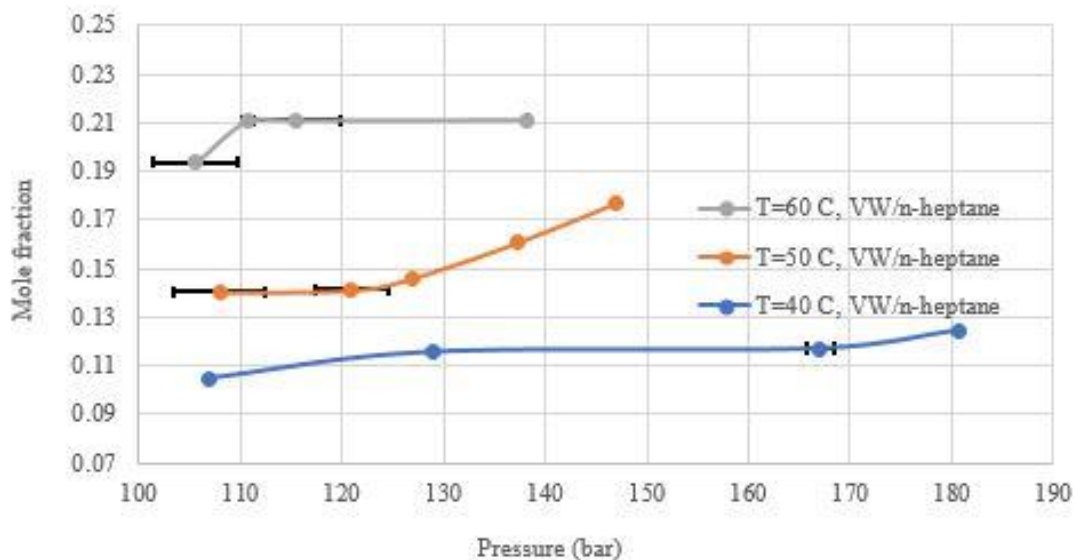


Figure 4.4 Mole fraction of VW/n-heptane dissolved in scCO₂ at T=40, 50, and 60 °C. Mass quantities of VW were converted to moles using an average molecular weight of 720 (g/mol) provided by KOSTER KEUNEN.

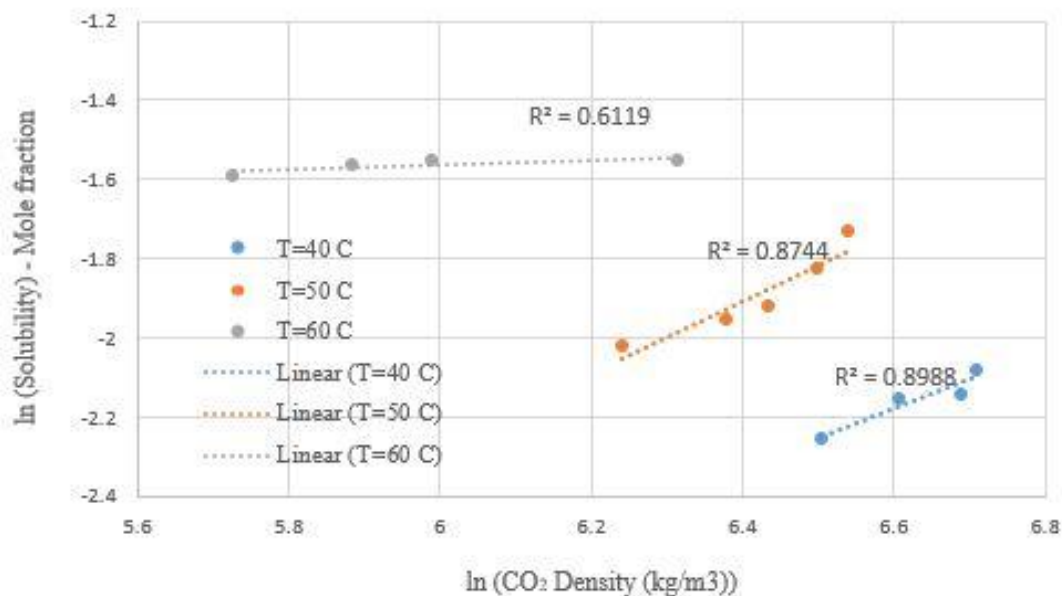


Figure 4.5. Relationship between ln Solubility and ln CO₂ density for VW/n-heptane solution in scCO₂.

As stated earlier plotting ln (solubility) versus ln (CO₂ density) can provide valuable confirmation of the solubility studies conducted in scCO₂ hydrophobic solution in scCO₂, based on the Chrastil equation [30]. The trend lines in Figure 4.5 demonstrate the existence of the linear relationship between the ln (solubility) and ln (CO₂ density) for temperatures of 40 and 50 °C, but this was not so noticeable at 60 °C. In all cases, the R² values were less than 0.9 (although 40 and 50 °C lines were close to this value), and they were all lower than those obtained with the AKD/n-heptane studies. The lack of more solubility data for this system at 60 °C and also larger experimental errors compared with the AKD/n-heptane solubility work can explain the lack of a better fit. However, the temperature trends are still observed, with higher temperature linear trends positioned higher on the ln(solubility) scale. The Chrastil equation is loosely observed, particularly at T = 40 and 50 °C.

4.1.3 Correlations between SCI at Cloud-Point Solubility Conditions for AKD/n-heptane/scCO₂, and Hydrophobic Development of Treated Paper

CA measurements were taken for treated paper substrates which were impregnated with AKD/n-heptane under solubility conditions obtained by cloud point experiment at different temperatures and pressures. For each impregnation process with AKD/n-heptane solution in scCO₂, two different solubility limits at T = 40, 50, and 60 °C were applied to impregnate the Whatman filter papers. Consequently, all CA measurements were executed for the impregnated papers with and without annealing temperatures (4h, T = 140, 160, and 180 °C). Conditions to prepare a paper substrate for the impregnation process are available in Table 4.3 and all measured mean CAs from day 0 to day 14 without annealing temperatures are shown in Figures 4.6-4.8.

Table 4.3. Conditions to impregnate the paper substrate with AKD/n-heptane solution and the subsequent annealing temperatures.

Conditions to prepare paper substrates			
T (°C) ± 1	P (bar)	Solubility (mL) ± 0.05	Annealing T (°C) ± 1
40	132.38	0.44	No
40	132.38	0.44	140
40	132.38	0.44	160
40	132.38	0.44	180
40	155.82	0.71	No
40	155.82	0.71	140
40	155.82	0.71	160
40	155.82	0.71	180
50	120.18	0.76	No
50	120.18	0.76	140
50	120.18	0.76	160
50	120.18	0.76	180
50	156.10	1.05	No
50	156.10	1.05	140
50	156.10	1.05	160
50	156.10	1.05	180
60	125.83	0.65	No
60	125.83	0.65	140
60	125.83	0.65	160
60	125.83	0.65	180
60	148.10	1.10	No
60	148.10	1.10	140
60	148.10	1.10	160
60	148.10	1.10	180

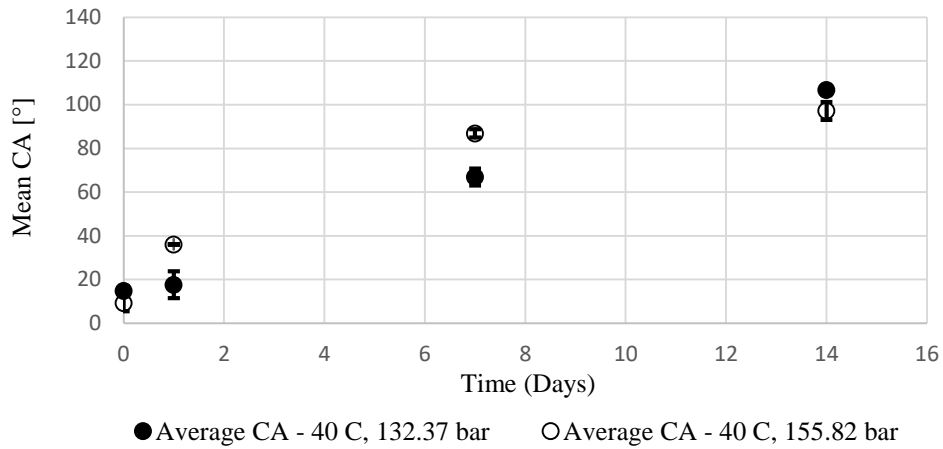


Figure 4.6. Mean CA VS days for the impregnated paper with AKD/n-heptane in scCO₂ at T=40 °C and two different pressures without annealing temperature.

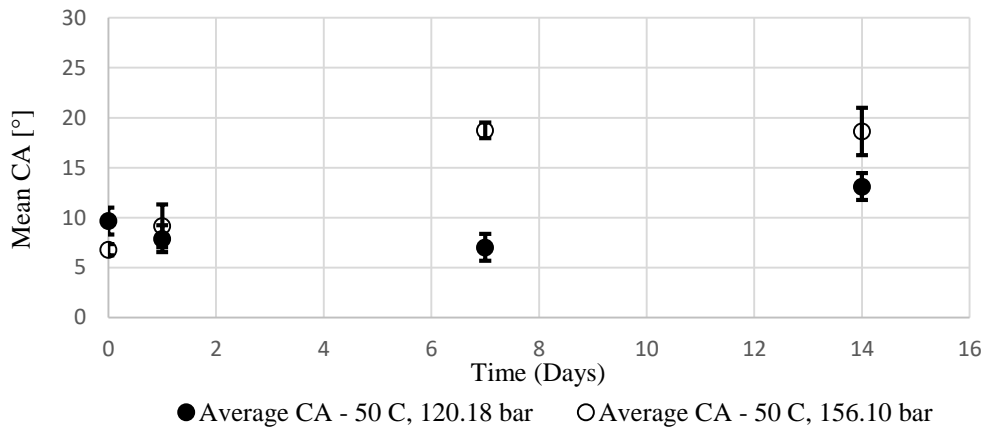


Figure 4.7. Mean CA VS days for the impregnated paper with AKD/n-heptane in scCO₂ at T=50 °C and two different pressures without annealing temperature.

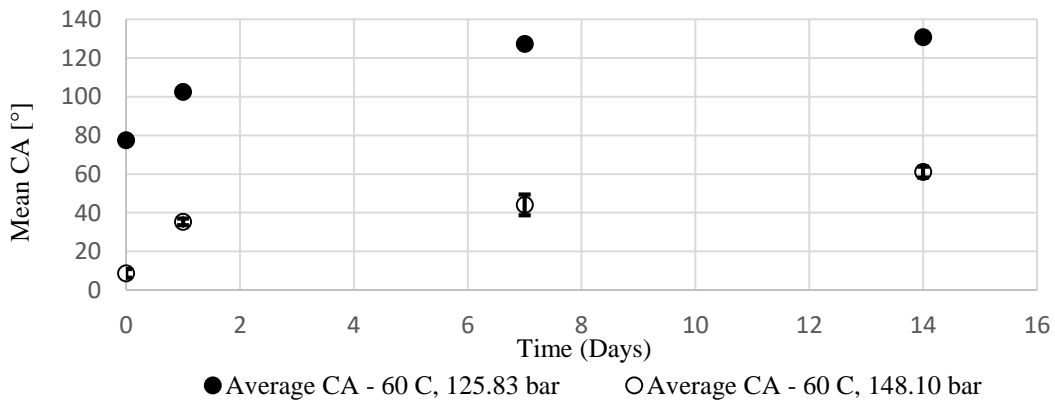
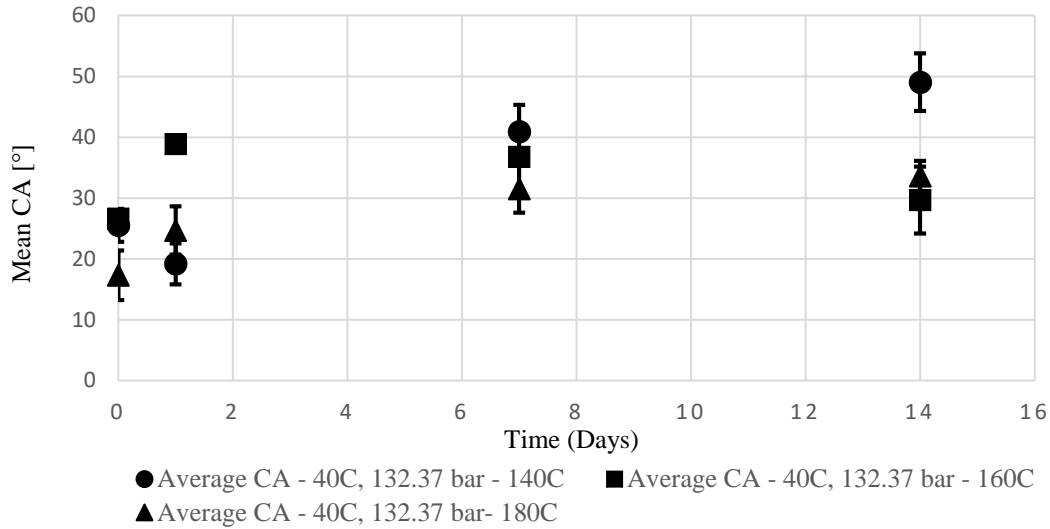


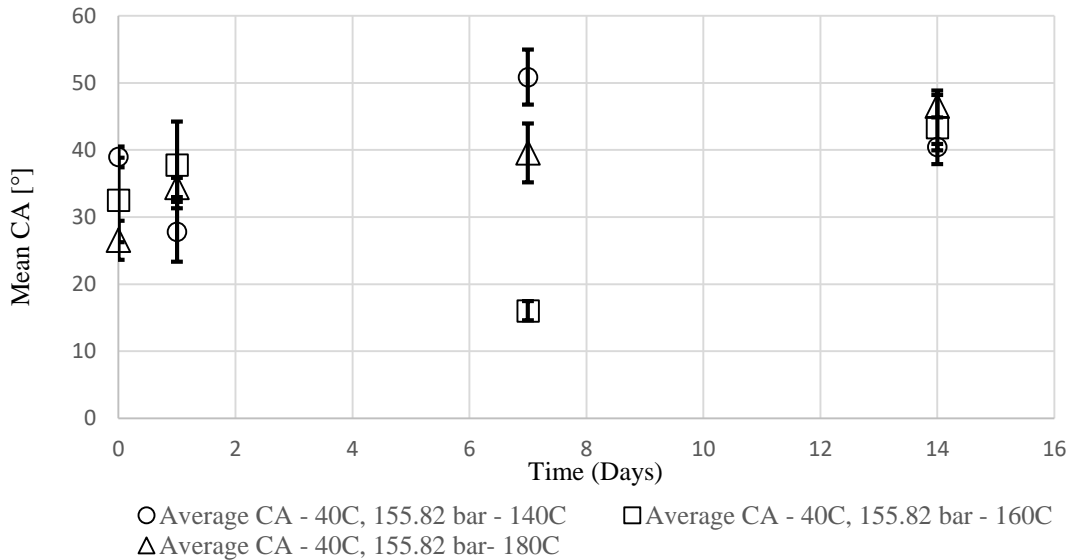
Figure 4.8. Mean CA VS Days for the impregnated paper with AKD/n-heptane in scCO₂ at T=60 °C and two different pressures without annealing temperature.

As illustrated in Figures 4.6-4.8, without annealing temperatures from day 0 to day 14 when T=40 and 60 °C CAs develop with time and on day 14 for T=40 °C and P=132.38 bar, mean CA is almost 106.70 ° and for T=60 °C and P=125.83 bar the average CA is 130.71 °. But, for T=50 °C, only for the lower pressure, P=120.18, CAs increase from day 1 to day 14 and when the pressure is 156.10 bar, first CA increases to 25.7 ° then decreases to almost 18.7 °. This confirms that although CAs develop with time, the condition in which the substrate has been prepared has an important role in the CA developing process. Among all three temperatures without annealing temperature, the highest CA achieved was at T=60 °C and P=125.83 bar. Therefore, this is the optimum condition that leads to an improvement in paper substrate hydrophobicity after modifications through impregnation processes in scCO₂ compared with T=40 and 50 °C.

Figures 4.9 – 4.11 show the progress of hydrophobic development via CA measurement from day 0 to day 14, with the added variable of annealing the impregnated samples at three different temperatures (140, 160, 180 °C). The annealing process/treatment affects modified paper roughness and was studied to see whether or not further improvements in hydrophobicity over the same period could be observed.



(a)

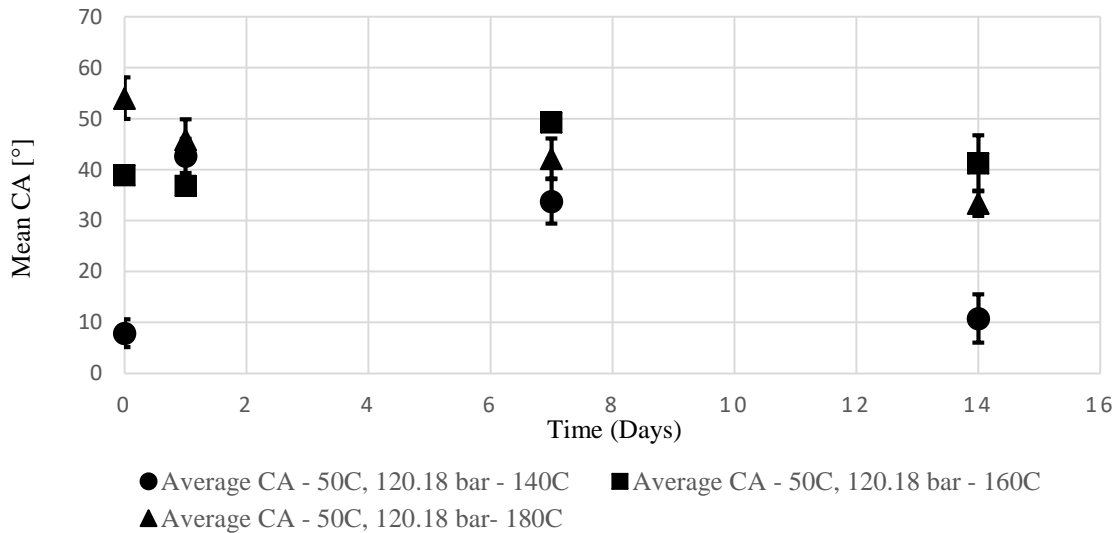


(b)

Figure 4.9. Mean CA measurements versus time for AKD-paper impregnated at $T=40\text{ }^{\circ}\text{C}$ and two different pressures with three annealing temperatures. (a) impregnated sample at a lower pressure and (b) impregnated sample at a higher pressure.

According to Figure 4.9, when $T=40\text{ }^{\circ}\text{C}$, drastic fluctuations in CAs belong to the higher pressure when the annealing temperatures are 140 and 160 $^{\circ}\text{C}$. For $T=40\text{ }^{\circ}\text{C}$ and $P=155.82\text{ bar}$ when annealing $T=140\text{ }^{\circ}\text{C}$, CA starts decreasing from 38.9 ° to 27.8 ° then starts increasing to 50.85 ° and decreases again. When $P=155.82\text{ bar}$ and the annealing $T=160\text{ }^{\circ}\text{C}$, there is a decrease

from 37.7 ° to 16.05 ° then an increase to 43.4 °. Moreover, for annealing T=180 °C, the trend of the CAs versus time is similar for both pressures, and at day 14 for the higher pressure, the measured CAs is almost 46.52 °. Although hydrophobicity with AKD addition develops with time [8], the effect of temperature and pressure on the impregnation process should be considered as well, and it is possible that T = 40 °C is not able to create good hydrophobicity for the paper substrate at the specified solubility conditions. Thus, collecting CA data from day 0 to day 14, and regarding the fact some areas of the paper substrates may have been covered with more AKD/n-heptane solution than others, the fluctuations in CA measurements are hence explained. Furthermore, hydrophobic AKD requires time to progress hydrophobicity throughout the whole paper area before it becomes uniform [8].



(a)

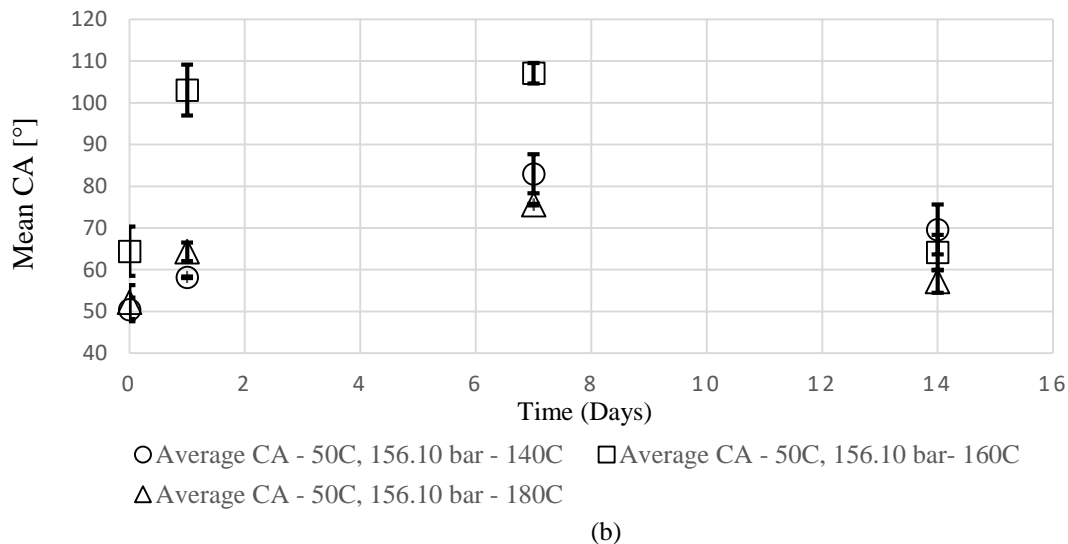
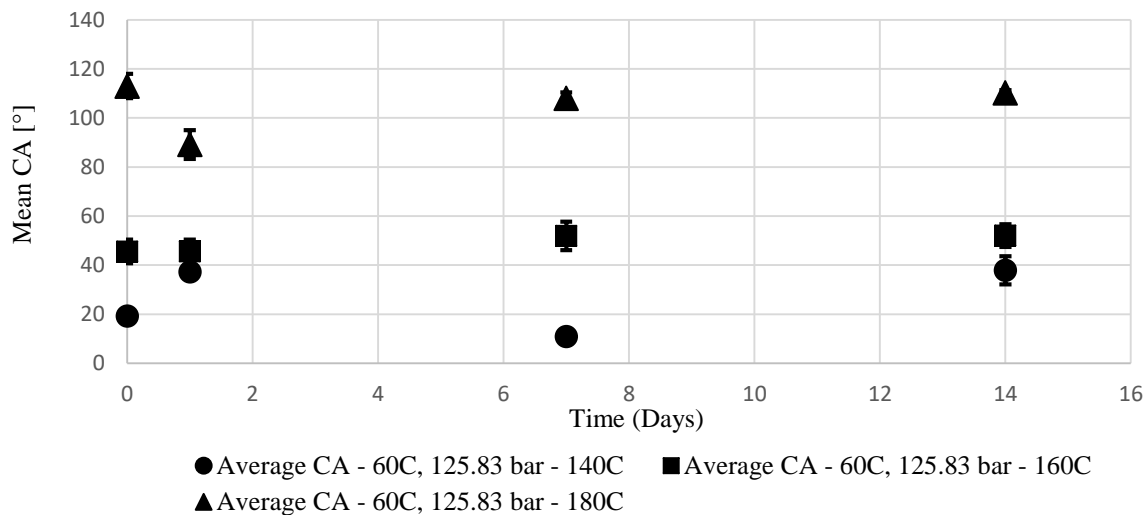
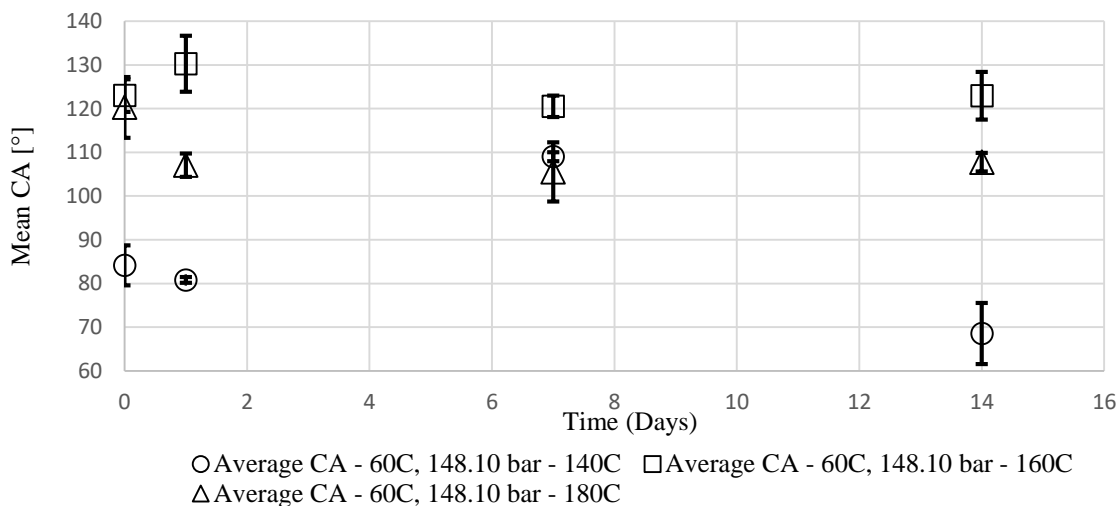


Figure 4.10. Mean CA measurements versus time for AKD-paper impregnated at $T=50\text{ }^{\circ}\text{C}$ and two different pressures with three annealing temperatures. (a) impregnated sample at a lower pressure and (b) impregnated sample at a higher pressure.

In Figure 4.10, there are still some fluctuations for CAs from day 0 to day 14. The worst condition for modifying a paper is $T = 50\text{ }^{\circ}\text{C}$, 120.18 bar and annealing $T=140\text{ }^{\circ}\text{C}$, which starts at CA of 7.91 ° then increases to almost 40 ° which possibly was measured at a specific spot of the paper, accumulated with more AKD and, subsequently after 14 days decreased to 10.79 ° . This points out the fact that at this particular condition no improvement was achieved on the surface of the paper. These same impregnation conditions, and the other two annealing temperatures of 160 and $180\text{ }^{\circ}\text{C}$ also show no overall progress from day 0 to day 14, deposit improvements in CA at intermediate time. Moreover, for 156.10 bar and annealing temperature of $180\text{ }^{\circ}\text{C}$, the CA started at 53.24 ° for day 0, increased to 75.58 ° at day 7 and at day 14 decreases to 57.17 ° . In general, applying solubility conditions for temperature $50\text{ }^{\circ}\text{C}$ and both low and high pressure was not able to provide favorable CA measurement considering developing of the hydrophobic solution by time.



(a)



(b)

Figure 4.11. Mean CA measurements versus time for AKD-paper impregnated at $T=60\text{ }^{\circ}\text{C}$ and two different pressures with three annealing temperatures. (a) impregnated sample at a lower pressure and (b) impregnated sample at a higher pressure.

According to Figure 4.11 for impregnation conditions at the highest temperature investigated ($T=60\text{ }^{\circ}\text{C}$) as shown in Figure 4.11 (b), the highest and the most stable CA measurements are for the annealing temperature of $160\text{ }^{\circ}\text{C}$ and 148.10 bar . A similar trend for CA development with a much lower CA, $37.90\text{ }^{\circ}\text{C}$ belongs to 125.83 bar when the annealing temperature is $140\text{ }^{\circ}\text{C}$. For the highest annealing temperature, $180\text{ }^{\circ}\text{C}$, and both pressures

investigated, there is no significant change from day 0 to day 14, and their progressing trend is similar from day 7 to day 14. Stable CA development is observed in this time region. The only condition that decreases at day 14 is when the annealing temperature is 140 °C and P=148.10 bar.

Considering all different conditions, it can be concluded that for impregnated papers without annealing treatment, at T=60 °C and lower P, (125.83 bar) the highest CAs were observed with time. But, for the other impregnation temperatures, only T=40 °C with the lower pressure of 132.37 bar at day 14 resulted in the measured CAs being > 100 (106.69 °). So, without annealing temperatures, impregnated paper at T=60 °C and 125.83 bar provided better hydrophobicity during this period. Moreover, annealing treatments at three different temperatures on modified paper substrates demonstrated that for the impregnated papers at T=60 °C and 148.10 bar with the annealing temperature of 160 °C the most hydrophobic paper substrate was generated with a CA of 122.95 °. Additionally, at this condition an appreciable hydrophobicity was created immediately after treatment and CAs are almost stable from day 0 to day 14.

SCI processes are assumed to uniformly distribute throughout the paper substrates, and while this assumption is desirable, paper porosity is random and deposits would be randomly distributed within these pores. Hydrophobicity develops slowly with the AKD movement throughout the paper substrates [8]. Since small portions were cut from the impregnated samples for CA measurements, it is possible that particular spots/regions were not yet covered by AKD. Also, it is possible that regions containing AKD deposits did not have enough time to spread to other parts of the paper fibers at a given measurement time. Therefore, the effects of chosen conditions from solubility measurements and subsequent annealing plus slow progression and movement of AKD throughout the paper matrix, help explain the fluctuations in CA measurements at different conditions with annealing temperatures.

Finally, the amount of AKD/n-heptane solution that impregnated into the paper fibers after supercritical impregnation was determined by weighing the paper before and after the impregnation process. The maximum amount that can be dissolved in scCO₂ should be proportional to the amount that can be impregnated into paper substrates for surface modifications. Table 4.4 shows the amounts which are expected to be impregnated into a paper substrate based on the concentration of AKD dissolved from solubility experiments, and also the amounts which have been measured after the impregnation process. The measured masses in Table 4.4 are close to the maximum amount that is expected to be dissolved in scCO₂. Figure 4.12 exhibits the actual amount of AKD/n-heptane solution impregnated into the paper substrates at different CO₂ densities.

Table 4.4. AKD mass impregnated into the paper substrates and CO₂ density at different conditions.

T (°C)	P-(bar)	CO ₂ Density (g/cm ³)	Expected mass impregnated determined from solubility (g)	Actual amount impregnated, gravimetric measurement (g)±0.0001
40	132.38	0.7482	0.0008	0.0006
40	155.82	0.7890	0.0013	0.0009
50	120.18	0.5858	0.0014	0.0010
50	156.10	0.7139	0.0019	0.0014
60	125.83	0.4774	0.0012	0.0010
60	148.10	0.5968	0.0019	0.0015

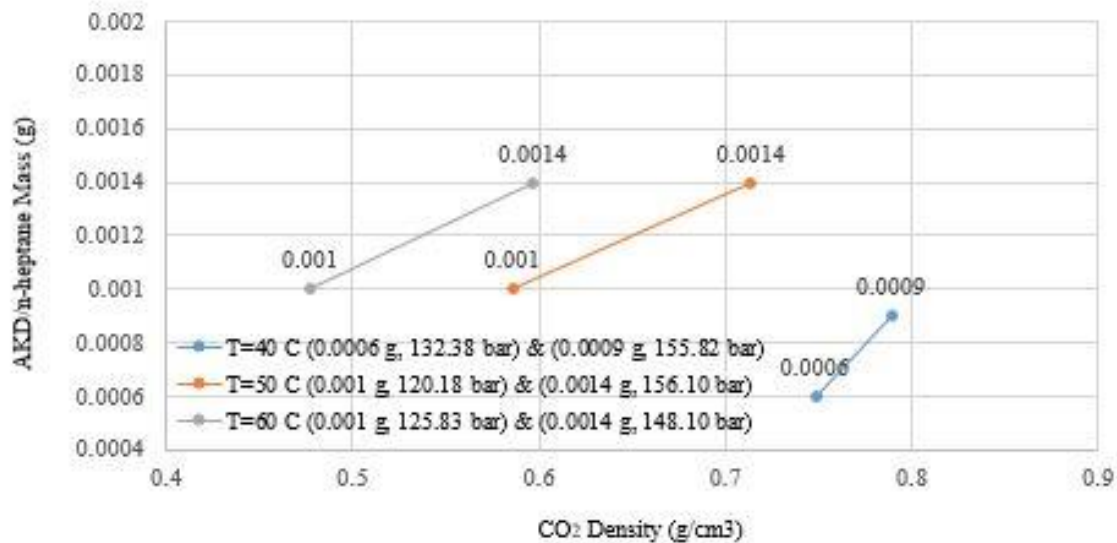


Figure 4.12. Actual AKD/n-heptane mass impregnated into the paper versus pure CO₂ density.

According to Figure 4.12, the higher the pressure for all three temperatures, the more AKD/n-heptane solution dissolved in scCO₂. CO₂ density decreases by increasing the temperature, Figure 4.12 clearly shows when CO₂ density is low, for instance at approximately 0.47 (g/cm³), 0.001 g of the hydrophobic solution is dissolved in scCO₂ at T=60 °C for P=125.83 bar and to have the same amount being dissolved in scCO₂ at T = 40 °C, the density of CO₂ should be almost 0.79 (g/cm³). Moreover, for each temperature, increasing the CO₂ density allows more AKD/n-heptane to be dissolved in scCO₂ at low and high pressures.

4.1.4 Effects of Impregnation and Annealing on the Paper Surface

To assess the physical changes occurring on the paper samples after impregnation and annealing, a selected set of conditions were chosen for SEM imaging, at 18 days after preparation. Two solubility conditions were chosen at approximately constant pressure but two different temperatures as described in Table 4.5, and samples were tested with and without annealing (T=160 °C, 4h). Comparisons focused on the effect of annealing at constant T and P impregnation conditions, and also the effects of impregnation temperature at constant P and annealing conditions. Moreover, SEM micrographs of untreated paper and those impregnated with excess amounts of AKD/n-heptane solution at room temperature [8] were compared with the present images to draw conclusions on suitability of impregnation conditions.

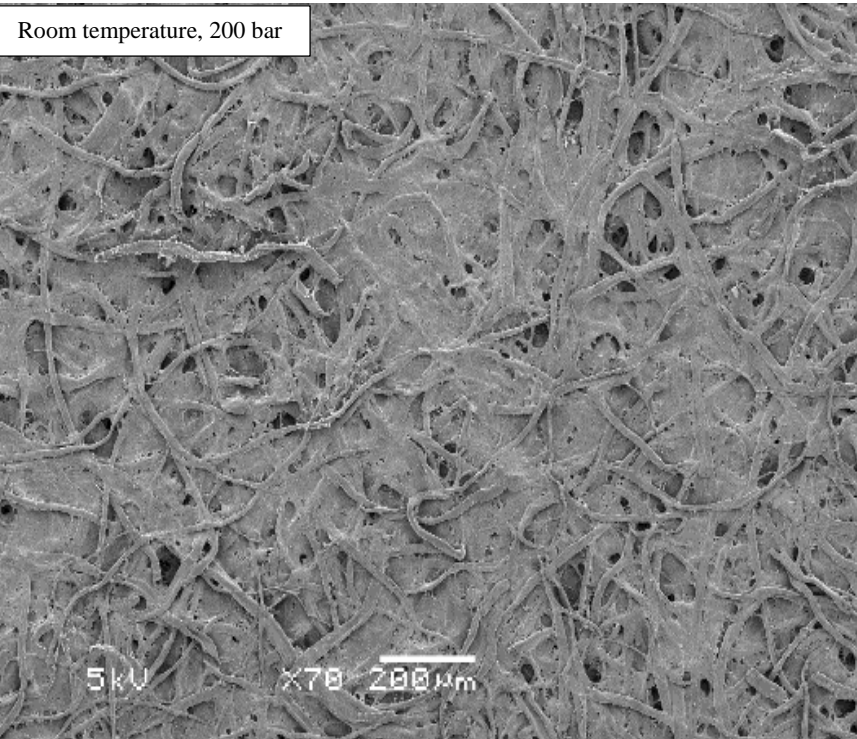
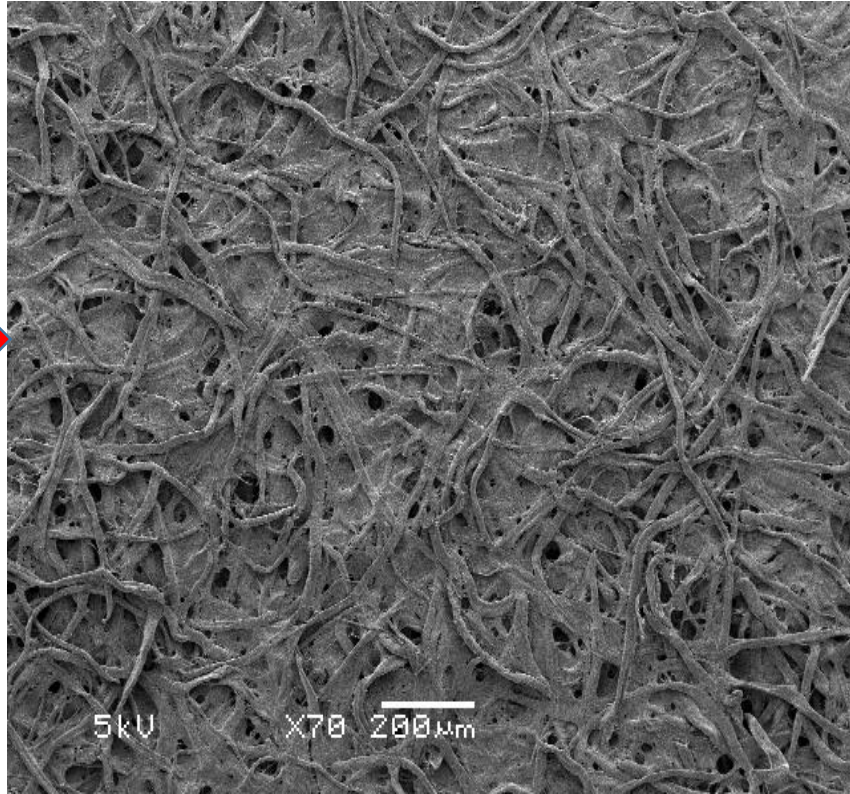
Table 4.5. Impregnation process conditions for preparing the paper substrates in scCO₂. Also shown is the measured CA at day 14 for these conditions (assumed approximately constant from Day 14 onwards), and short descriptions of the samples based on SEM observations.

Samples	Temperature (°C)	Pressure (bar)	Annealing T (°C)	CA at day 14 (°)	Observations
1	40	155.82	160	43.31	High porosity
2	40	155.82	NO	97.17	High roughness
3	50	156.10	160	64.17	Low porosity, low-scale roughness
4	50	156.10	NO	18.63	High porosity, high-scale roughness

For the untreated paper, the SEM image shows significant porosity (Figure 4.13 a), but in Figure 4.13 b, the SEM image shows several of the substrate pores now filled in with AKD. This condition was performed at room temperature and 200 bar, excess AKD/n-heptane added (well beyond the solubility limit) and 10 days after impregnation [8]. AKD spread over the cellulose fibers during this time period, and created a more uniform surface with less pores and likely higher micro-roughness as judged by the improvement in CA during this time, which was 129° [8].

SEM images compared the changes in the structure of the impregnated paper substrates before (Figure 4.13 c and e) and after (Figure 4.13 d and f) annealing at 160°C for 4 hours, low and high magnification respectively. The impregnation conditions were $T=40^\circ\text{C}$ with $P=155.82$ bar. For the first sample lower magnification images (Figure 4.13. c-d) both show a more porous structure on the surface of the paper. At the higher magnification, (Figure 4.13. e-f), a substantial change in morphology of the paper is observed, as is a more even distribution of AKD through the matrix of the paper. More pores are visible at the surface of the paper substrate in the annealed samples with diameters bigger than $5\ \mu\text{m}$, while the non-annealed samples show relatively large wave-like wax deposits to a size of less than $1\ \mu\text{m}$.

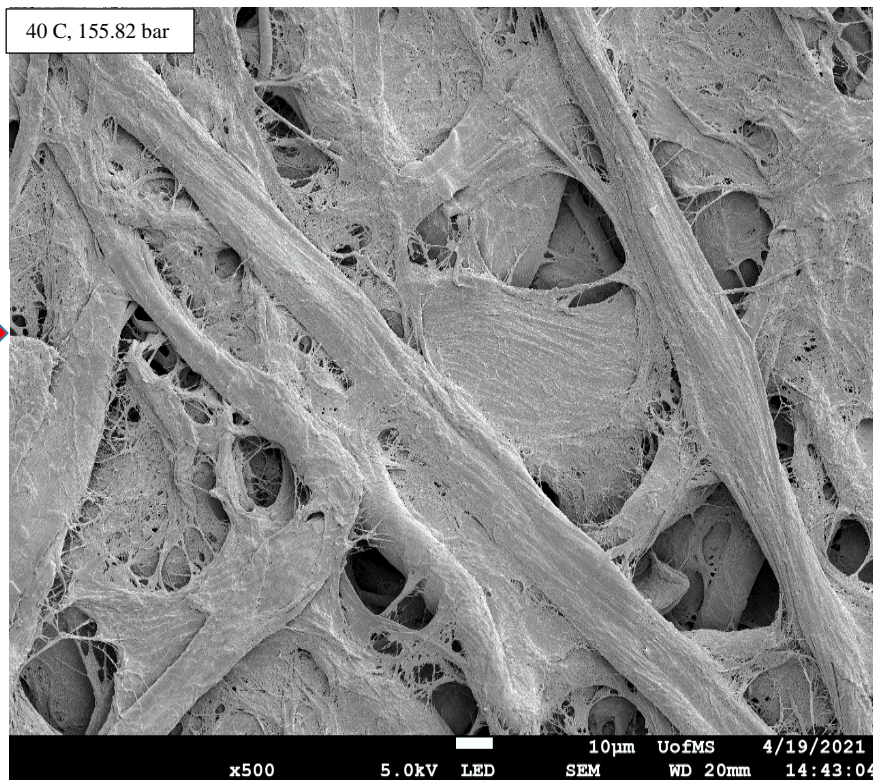
a) Plain Paper



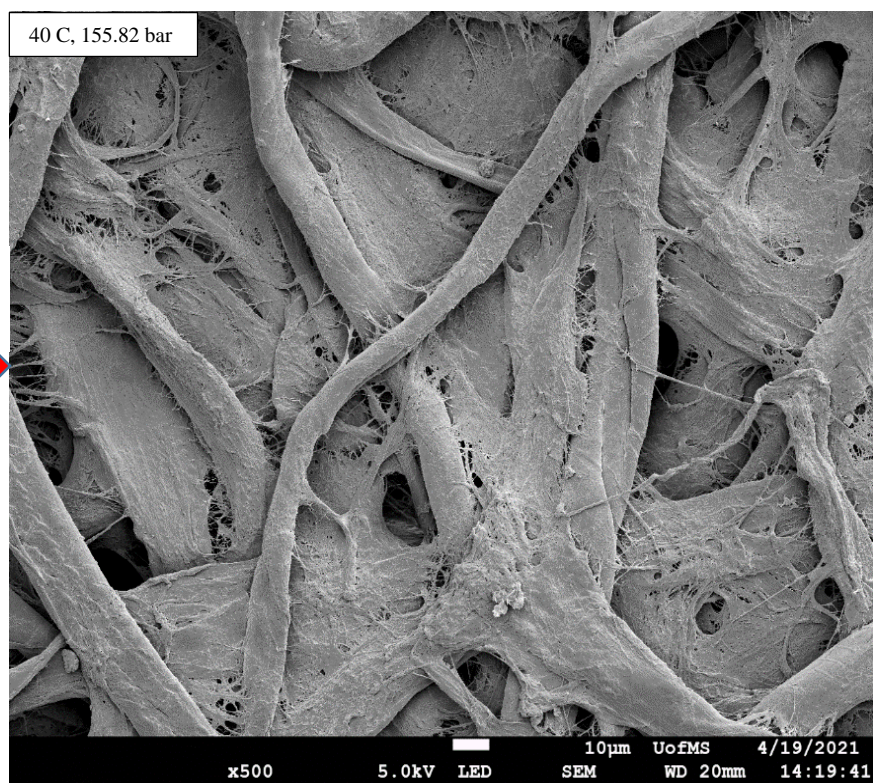
b) Impregnated



c) Impregnated

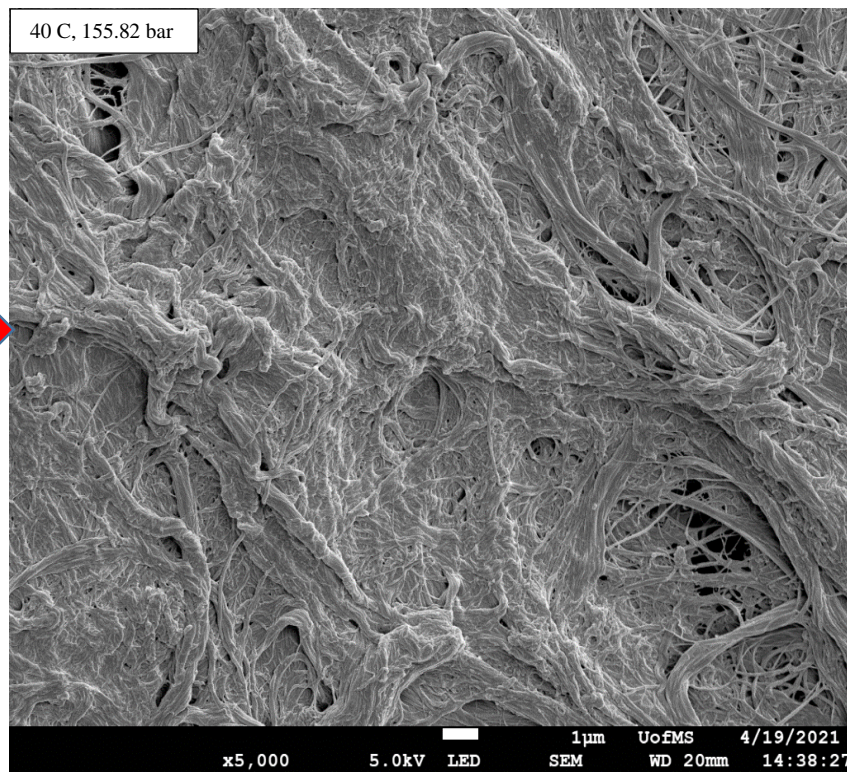


d) Impregnated
and Annealed

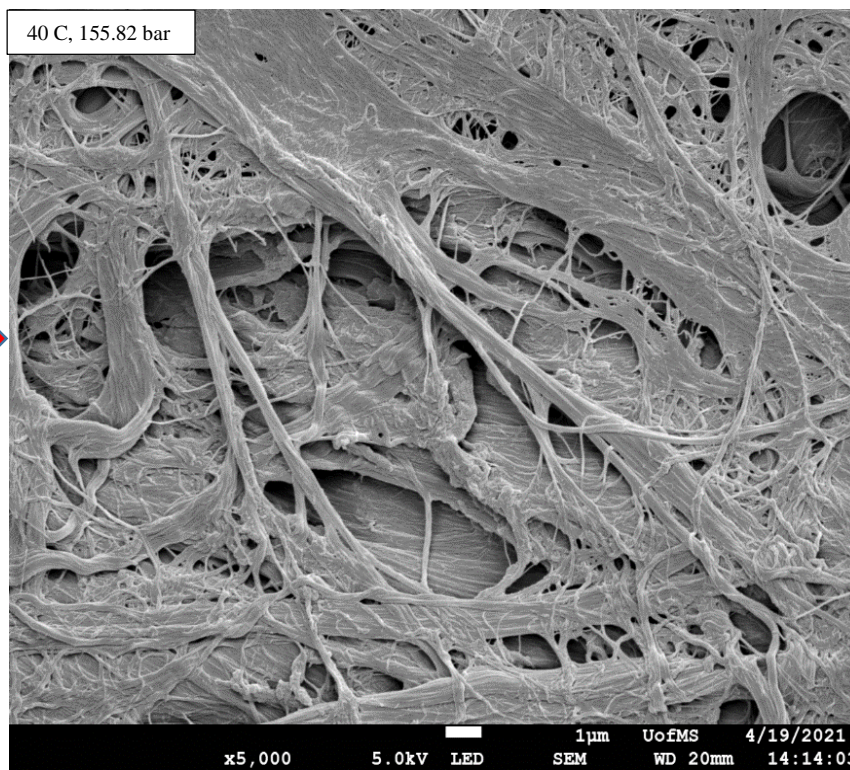


Low magnifications (x 500)

e) Impregnated
→

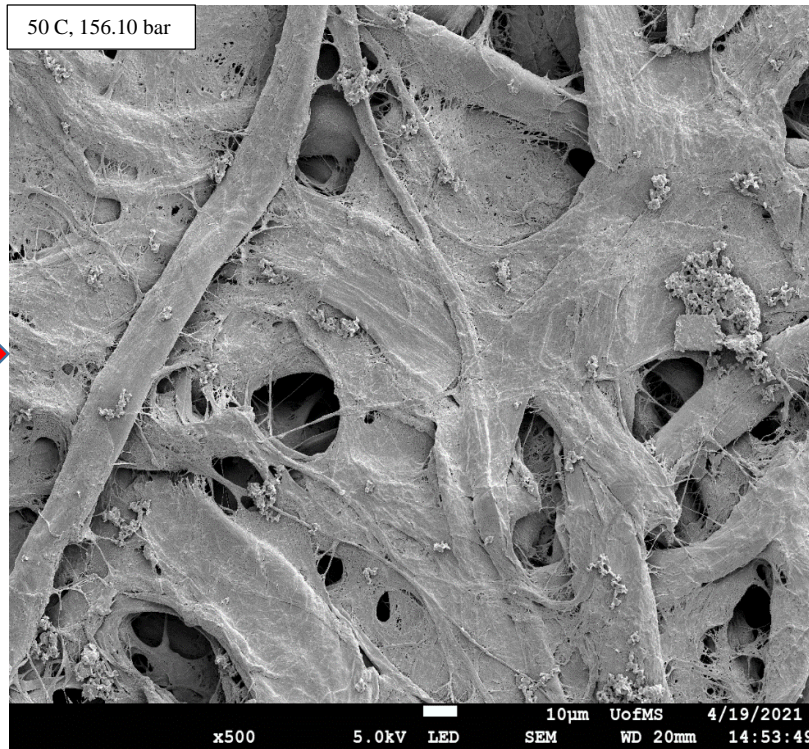


f) Impregnated
and Annealed
→

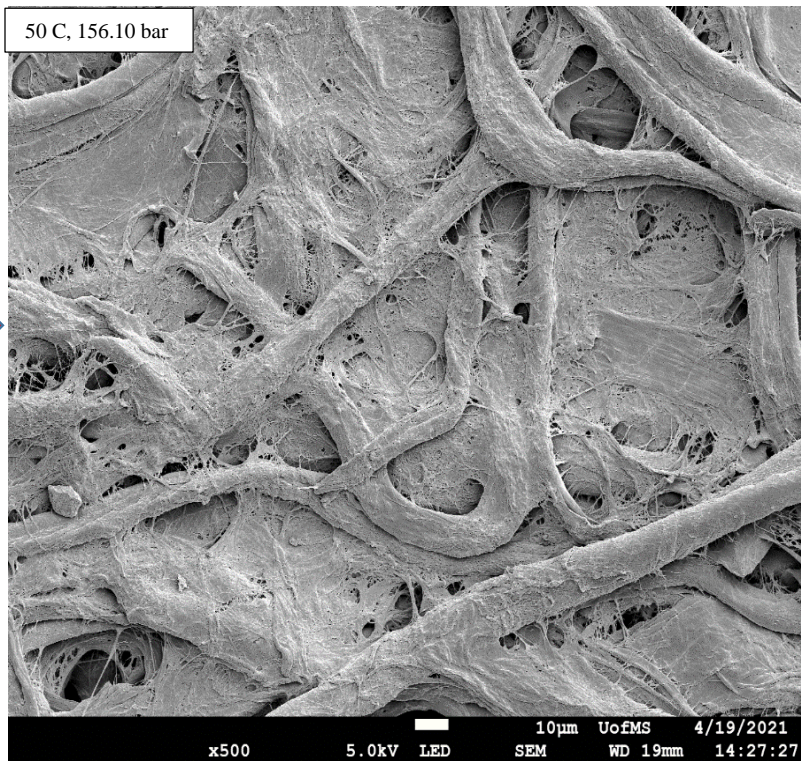


High magnifications (x 5000)

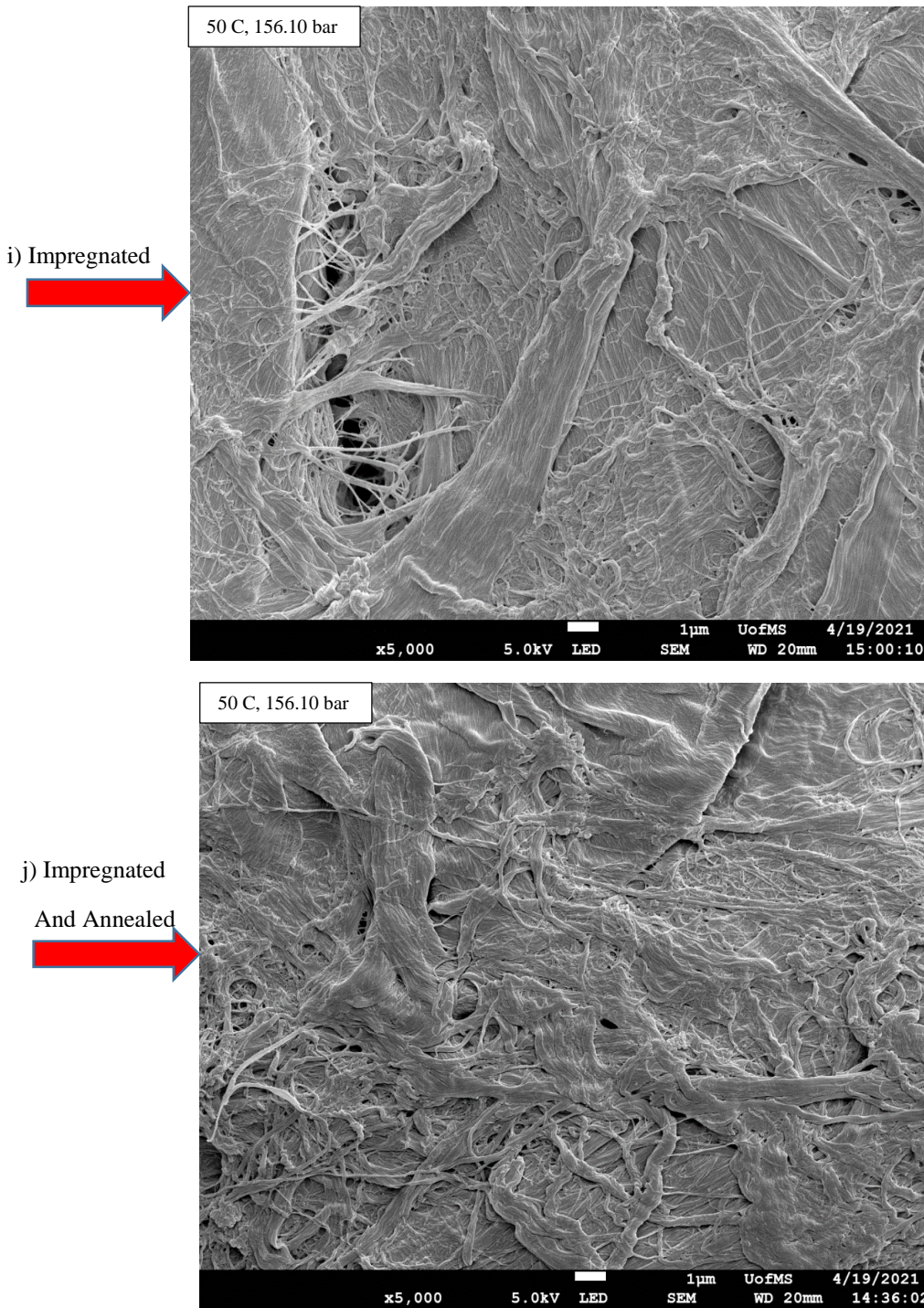
g) Impregnated



h) Impregnated
and Annealed



Low magnifications (x 500)



High magnifications (x 5000)

Figure 4.13. SEM micrographs of (a) plain paper and (b) AKD-impregnated paper with (an excess amount of AKD/n-heptane solution), impregnated at room temperature and P=200 bar, after 10 days [8]. SEM images (c-f), AKD-impregnated papers (1.8 g/L, T = 40 °C, P=155.82 bar), before and after annealing (4 h, 160 °C). Images (g-j) AKD-impregnated papers (1.8 g/L, T = 50 °C, P=156.10 bar), before and after annealing (4 h, 160 °C). low magnifications (c-d, g-h) and high magnifications (e-f, i-j) show the morphology and structure of the paper substrates for T = 40 and 50 °C.

SEM images Figure 4.13 (g-j) belong to the sample impregnated at ($T = 50\text{ }^{\circ}\text{C}$ and $P=156.10\text{ bar}$) before (g and i) and after (h and j) annealing. In the low magnification images, large deposits on the surface of the paper substrate are observed before annealing, while a more uniform distribution of AKD through the matrix of the paper substrate is observed after annealing. In the high magnification images, there are fewer wavy-like structures in the impregnated sample compared with the equivalent sample at $T = 40\text{ }^{\circ}\text{C}$ impregnation temperature, and also more pores. After annealing, there appear to be far fewer pores than that observed in the $40\text{ }^{\circ}\text{C}$ case. Also, for the annealed sample, only a small quantity of similar-shaped deposits are left on the surface but the predominant part is continuously uniform and stringy which favors higher contact angles.

Roughness on the surface contributes to improved hydrophobicity [4]. These SEM images indicate that roughness can be influenced by the impregnation process conditions. Therefore, it is essential to choose the most appropriate temperature and pressure for the paper substrate impregnation process and the subsequent annealing temperature to optimize the surface roughness as well as the quantity of AKD impregnated. SEM images revealed that the sample impregnated at $T = 40\text{ }^{\circ}\text{C}$ and without annealing (c and e) are more uniform and a continuous surface was created. On the other hand, better micro-roughness (h and j) and higher CAs were achieved after annealing (4h , $160\text{ }^{\circ}\text{C}$) for the AKD/n-heptane impregnation into paper substrates in scCO_2 at $T=50\text{ }^{\circ}\text{C}$.

The various impregnation and annealing conditions used to prepare the hydrophobic paper resulted in surfaces with modified porosity and roughness, and changes to these two parameters influences the resulting CA as described by the Cassie-Baxter equation (p. 9). Generally speaking, a hydrophilic surface with a theoretical smooth CA of $< 60^{\circ}$ can increase its CA with the addition

of low roughness and high porosity to the surface [33]. Addition of high roughness and low porosity can actually make an initially hydrophilic surface even more hydrophilic (i.e. lower CA).

Referring again to the SEM images in Figure 4.13 and the approximate CA observed at these conditions (given in Table 4.5), qualitative conclusions linking the observations to the Cassie-Baxter equation may be made. Comparing the impregnated-only samples, the higher impregnation temperature resulted in larger-scale roughness, and the Day 14 CA was considerably less than that impregnated at 40 °C. Considering the annealed samples, the higher impregnation temperature condition resulted in the presence of smaller-scale roughness, which provided a higher Day 14 CA than the 40 °C impregnated case. Lastly, the effects of annealing vs no annealing at constant impregnation conditions (T and P) showed inconclusive results, with annealing reducing the hydrophobic effects in one case and improving it in the other case.

Finally, the impact of using solubility limits to impregnate AKD/n-heptane into paper substrates (with or without annealing) vs excess impregnation of the wax at room temperature and no subsequent annealing is considered. Using solubility limits to impregnate the paper with AKD/n-heptane showed that at 40 °C without annealing the CA is almost 97 ° with an even distribution of AKD throughout the substrate. But for the higher temperature, 50 °C the progress in hydrophobicity was observed after annealing process with a CA of 64.17 °, Table 4.5. Moreover, the paper impregnated at room temperature and 200 bar with an excess amount of the AKD/n-heptane showed the CA of 129 ° with less pore size area, 10 days after impregnation [8].

4.2 Design Results

4.2.1 Design of Experiment (DOE)

Design of experiment (DOE) is a powerful and useful statistical tools in product design that helps to analyze data more efficiently. DOE can be applied in various areas including but not limited to design optimization, variable identification, process control and improvement, and, product performance prediction. Statistical analysis regarding the ANOVA method (e.g. ANOVA table in DOE), provides valuable information for experimenters in conducting future experiments in a variety of research areas [34, 35].

Designed experiments play significant roles in innovation and process improvements [34]. The experimenter initially considers the goal of the experiment, identifies what should be measured accurately the “response values” [35]. Also, constant factors which cannot be changed during the actual experiment should be considered as well. Choosing an appropriate model which adequately describes the physical situation is essential. DOE provides platforms that guide an experimenter to specify response factors constraints and interactions.

The user can generate the design by applying input variables and then reviewing and evaluating the final results to understand its strength and limitations to ensure it provides the goals and information required. Finally, data will be collected from the experiments and the response value recorded for each trial. Sometimes a user has to augment the design to resolve possible ambiguities. By completing all design steps, graphs and tables are provided by the Design-Expert software (Version 12) for the user to analyze and compare predicted results obtained by DOE with experimental results from laboratory work.

4.2.2 Design Objectives and Factors Affecting the Experimental Design

Design Expert was used to develop an experimental program for the cloud point solubility experiments to determine the maximum solubility of wax/n-heptane in scCO₂ at different temperatures and pressures. ANOVA methods and design graphs were subsequently employed within the software to confirm the validity of the lab results for cloud point pressures.

4.2.3 Factors for Cloud Point Experiment Designs

In general, the following factors may affect the cloud point experiment in scCO₂.

1. Cell temperature
2. Cell pressure
3. Volume of wax/n-heptane solution
4. Wax/n-heptane solution density

Choosing the appropriate main factors that are involved in the experiment is an important step, and by *factor screening* these above factors for a *closed system* are as follows:

1. Cell temperature (°C)
2. Wax/n-heptane solution (mL)

4.2.3 AKD/n-heptane Cloud Point Pressure Design

In this DOE, the goal is predicting the cloud point pressure for the solubility of AKD/n-heptane in scCO₂ using Design-Expert and consequently analyzing the predicted results obtained by DOE. There are two categoric factors which have two discrete levels: temperatures and wax/n-heptane quantities; and the pressure is the dependent variable which is adjusted until the cloud point is observed (see Tables 4.6 and 4.7). Therefore, an appropriate design which is “Multilevel Categorical Design” was chosen and all analyses were based on that design. The controllable factors are the ME identified above (cell temperatures and volumes of the AKD/n-heptane solution), while “Cloud Point Pressure” is the “Response Value”.

Table 4.6. Multilevel Categorical Design factors and levels for AKD/n-heptane.

	Name	Unit	Level	L (1)	L (2)	L (3)	L (4)
A (Categoric)	Temperature	C	3	40	50	60	-
B (Categoric)	AKD/n-heptane	mL	4	0.128	0.173	0.203	0.233

Table 4.7. Multilevel Categorical Design factors and response value for AKD/n-heptane.

Standard run order	Run	Factor 1: A-Temperature	Factor 2: B-AKD/n-heptane	Response Value: Cloud Point Pressure
11	1	50	0.233	13.68
7	2	40	0.203	15.68
5	3	50	0.173	12.42
8	4	50	0.203	12.99
2	5	50	0.128	11.8
1	6	40	0.128	13.05
12	7	60	0.233	13.22
9	8	60	0.203	12.69
3	9	60	0.128	11.6
4	10	40	0.173	14.62
10	11	40	0.233	16.73
6	12	60	0.173	12.22

Since there are some limitations in applying the software, such as low and high boundaries for input variables, collected raw data needed to be fitted in Excel and the corresponding pressures were being calculated from the fitted equation. For this purpose, cloud point pressure (Y-axis) was graphed versus AKD/n-heptane solution (mL). The fitted data are available in table 4.8.

Table 4.8. Quantities of AKD/n-heptane dissolved in scCO₂ at T = 40, 50, and 60 °C.

Temperature (°C)	AKD/n-heptane solution (mL)	Response: Pressure (MPa)
40	0.1280	13.05
40	0.1730	14.62
40	0.2030	15.68
40	0.2330	16.73
50	0.1280	11.80
50	0.1730	12.42
50	0.2030	12.99
50	0.2330	13.68
60	0.1280	11.60
60	0.1730	12.22
60	0.2030	12.69
60	0.2330	13.22

The pressure values were fitted to AKD/n-heptane solution values based on raw data obtained. The fitted equations were $35X+8.5698$ with $R^2=0.9859$ for T = 40 °C, $64.791X^2-5.324X+11.403$ with $R^2=0.9853$ for T = 50 °C and $28.213X^2+5.1617X+10.482$ with $R^2=0.9912$ for T = 60 °C.

At this stage, all data have the same boundaries which are compatible with the criteria of Design-Expert software. Therefore, “Multilevel Categorical Design” was chosen for this DOE and consequently used in the analysis of predicted results. In this design, factor A (temperature) has three levels, and factor B (amount of AKD/n-Heptane solution) has four levels. The half-Normal Plot shows that both factors A and B are significant in Figure 4.14.

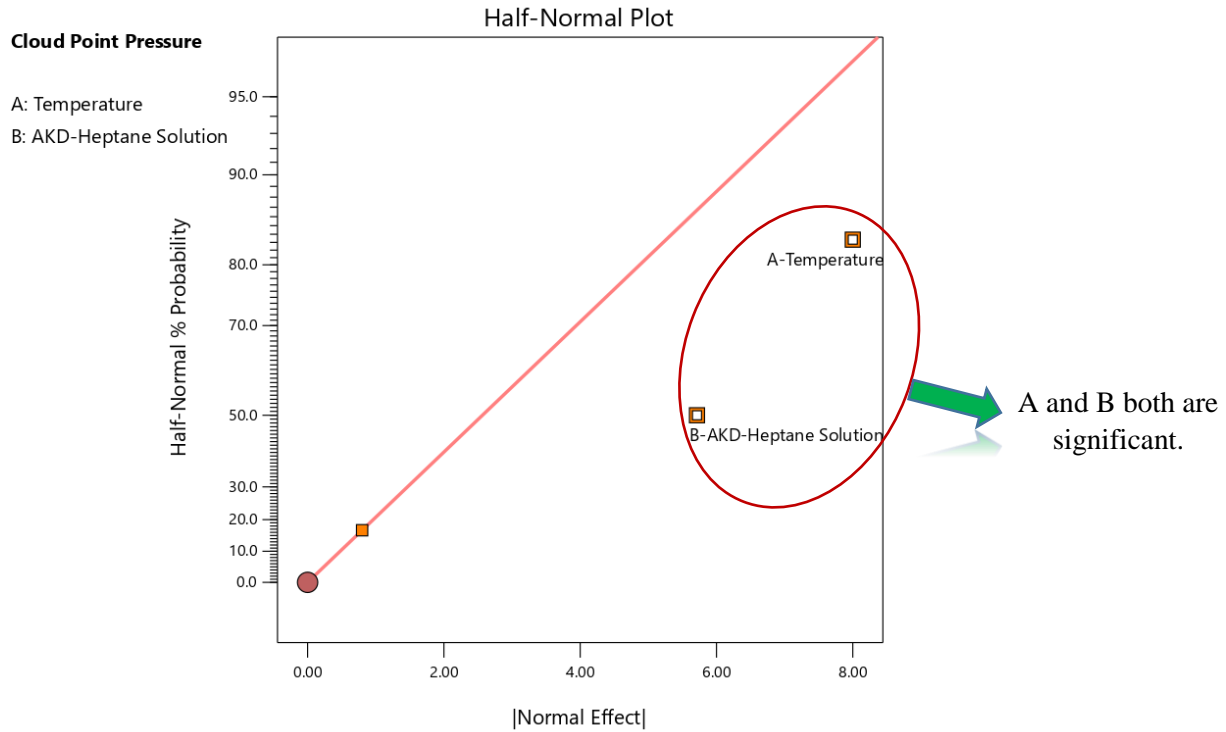


Figure 4.14. Half-Normal Plot from Design-Expert for AKD/n-heptane solution in scCO₂.

After completing all input information in the Design-Expert, the software automatically chooses significant factors for the user as shown in Figure 4.14.

According to *ANOVA Table* from Design-Expert, the model is significant and both factors are significant as well, which is desirable. The term significant belongs to the model and both factors.

Table 4.9. ANOVA table from design-expert for AKD/n-heptane.

ANOVA for selected factorial model

Response 1: Cloud Point Pressure

Source	Sum of Squares	df	Mean Square	F-value	p-value	
Model	25.43	5	5.09	21.72	0.0009	significant
A-Temperature	16.08	2	8.04	34.33	0.0005	
B-AKD-Heptane Solution	9.35	3	3.12	13.31	0.0046	
Residual	1.40	6	0.2341			
Cor Total	26.83	11				

In the **Diagnostics** part, everything is satisfactory. Both graphs, Normal Plot versus Residual and also Residual versus predicted show the normality assumption is met and therefore are acceptable.

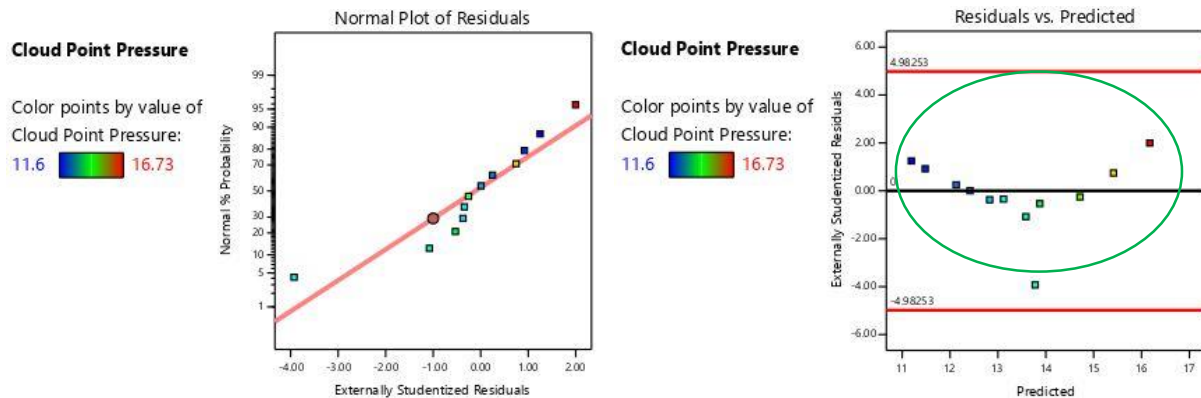


Figure 4.15. Normal plot of residual and residual versus predicted obtained from design-expert for AKD/n-heptane in scCO_2 .

The next step relates to **Model graphs** which provide complete information about all main factors and their interactions.

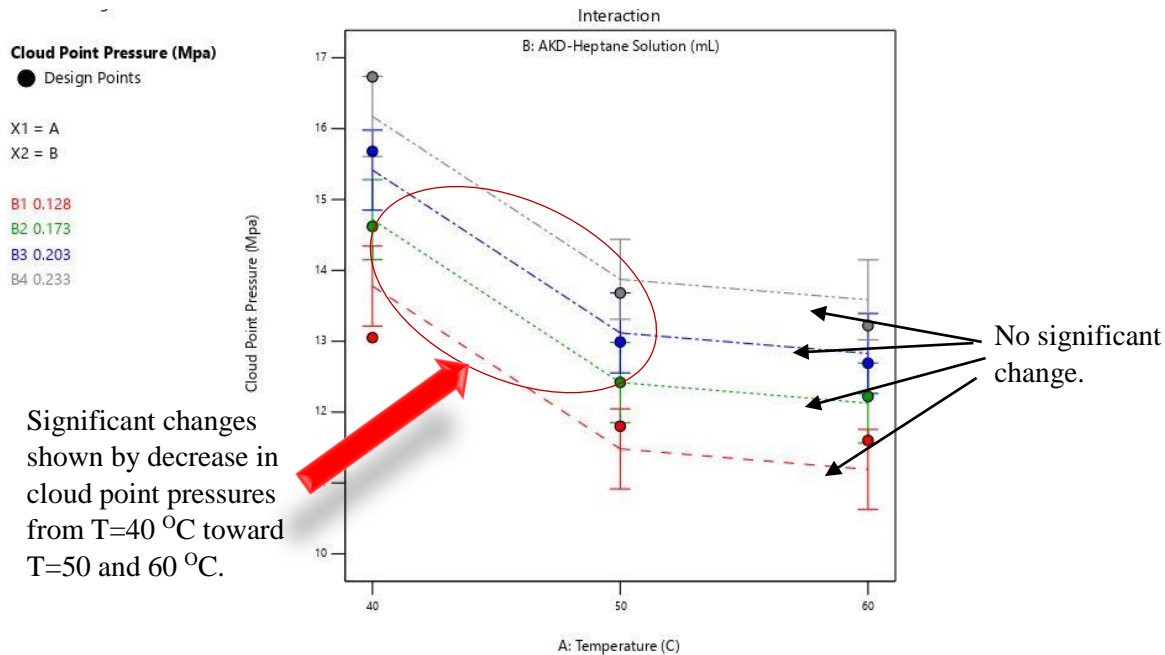


Figure 4.16. Interaction graph extracted from design-expert, for AKD/n-heptane cloud point pressure (MPa) versus temperature (°C).

As shown in Figure 4.16, one can see that at the lower temperature of 40 °C, higher pressure is needed to dissolve 0.2330 mL of AKD/n-heptane solution in scCO₂. Also, moving from T=40 °C toward T=50 or 60 °C, considering the position of least square difference (LSD) bars with their different colors, for example, red LSD bar at T=40 °C will not overlap with the red LSD bar which belongs to T=50 or 60 °C due to the considerable difference in the cloud point pressure. This fact proves a significant change in the solubility of the hydrophobic solution in scCO₂ at different temperatures. Another important point is that there is no significant difference between the cloud point pressures for T=50 and 60 °C. For instance, at B1=0.128 (sample solution mL) which is shown by a red dash in Figure 4.16, moving from T=50 °C toward T=60 °C there is only a slight decrease in the cloud point pressure. In addition, for all four different amounts of B (AKD/n-heptane solution), by changing the temperature from T=40 to T=50 and 60 °C a significant difference is observed which leads to a drastic drop in the cloud point pressure needed

to dissolve a specific amount of AKD/n-heptane solution (mL) in scCO₂. Furthermore, the design expert provides information for the interaction between factor A (temperature) and factor B (AKD/n-heptane solution) and also how they influence the cloud point pressure at different levels for all three temperatures. This is graphed in Fig 4.17.

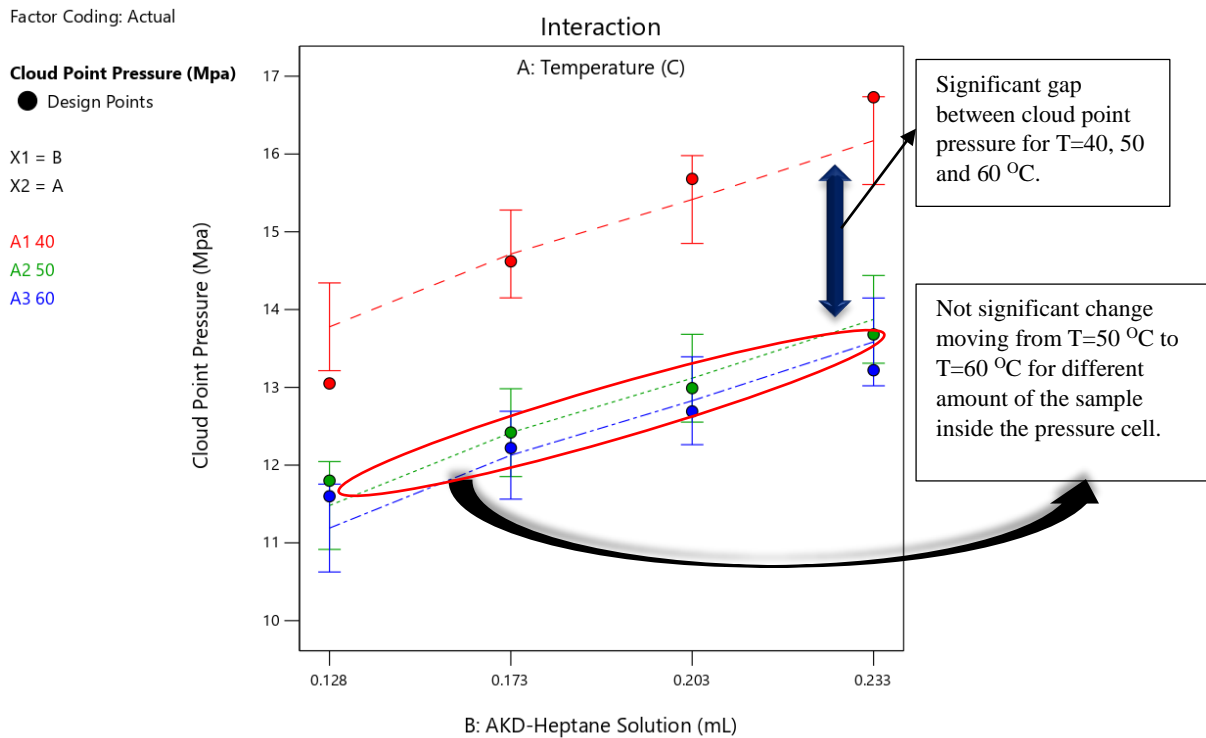


Figure 4.17. Interaction effect extracted from design-expert, for AKD/n-heptane cloud point pressure (MPa) vs solution (mL).

According to Figure 4.17, one can conclude that at a lower temperature ($T = 40\text{ }^{\circ}\text{C}$) higher pressures are necessary for dissolving the AKD/n-heptane in scCO₂. Also, all dash lines show by increasing the volume of the solution there is an increase in cloud point pressure and this increase starts from a higher pressure at a lower temperature which is $T = 40\text{ }^{\circ}\text{C}$ and the cloud point pressure is around 13.2 MPa. Furthermore, there is no significant difference in cloud point pressure for $T=50$ and $60\text{ }^{\circ}\text{C}$. The 3D Surface plot proves these observations, Figure 4.18.

Factor Coding: Actual

3D Surface

Cloud Point Pressure (Mpa)

Design Points:

- Above Surface
- Below Surface

X1 = B

X2 = A

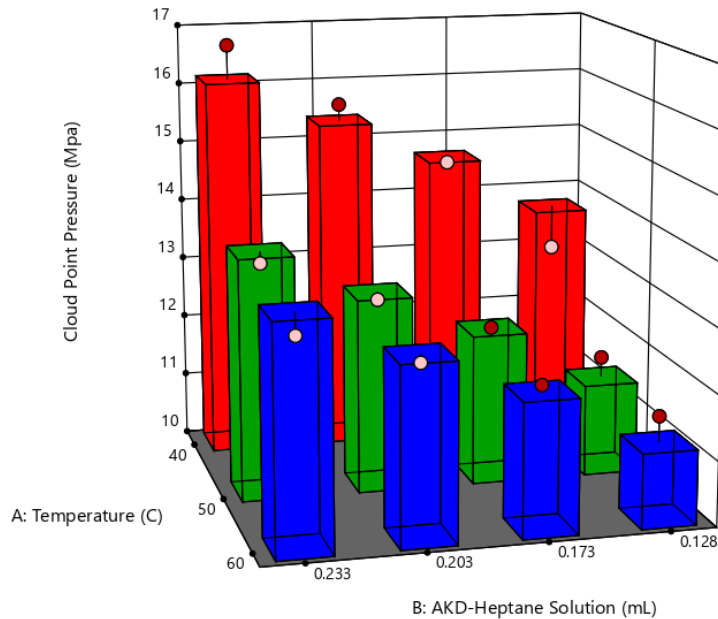


Figure 4.18. 3D surface plot from design-expert for AKD/n-heptane cloud point pressure (MPa) VS temperature and amount of AKD/n-heptane (mL).

The 3D surface plot clearly shows higher solubility of 0.233 mL of AKD/n-heptane is dissolved in scCO₂ at a lower pressure for T = 60 °C. Therefore, at lower cloud point pressures there is a maximum solubility of AKD/n-heptane solution in scCO₂ for higher temperatures. In addition, by decreasing the temperature from T = 60 °C to T = 40 °C for all volumes of AKD/n-heptane the high-pressure cell must be more pressurized to dissolve all AKD/n-heptane solution in scCO₂.

4.2.4 VW/n-heptane Cloud Point Pressure Design

As previously mentioned the first step after choosing the appropriate design is choosing the main factors. In this design, factors A (temperature), factor B (amount of VW/n-heptane), and AB (interaction) are all significant, as automatically chosen by the Design-expert software. If the user decides not to choose a specific factor, a **Warning Message** will be displayed which says “*largest effect not selected*”. In this study, there are three levels for temperatures (40, 50, and 60 °C) and three levels for the amounts of VW/n-heptane (mL) (0.65, 0.78 and 0.845). Table 4.8 shows the solubility data for the VW/n-heptane cloud point pressure design.

Similarly, as described with the AKD work, the main goal is to identify the trend of cloud point pressures of VW/n-heptane in scCO₂ and consequently analyzing the results obtained by DOE. “Multilevel Categorical Design” was also chosen and all analyses are based on this design. Controllable factors are cell temperatures and volumes of the VW/n-heptane solution; “Cloud Point Pressure” is the “Response Value”. Factors with their levels and also the response value are shown in Tables 4.10 and 4.11.

Table. 4.10. Multilevel Categorical Design factors and levels for VW/n-heptane.

	Name	Unit	Level	L (1)	L (2)	L (3)
A (Categorical)	Temperature	C	3	40	50	60
B (Categorical)	WV/n-heptane	mL	3	0.650	0.780	0.845

Table. 4.11. Multilevel Categorical Design number of runs, factors and the response value for VW/n-heptane.

Standard run order	Run	Factor 1: A- Temperature	Factor 2: B- VW/n-heptane	Response Value: Cloud Point Pressure
3	1	60	0.6500	10.86
15	2	60	0.8450	11.85
13	3	60	0.6500	10.27
6	4	60	0.7800	11.1
5	5	50	0.7800	11.84
12	6	50	0.7800	12.34
2	7	50	0.6500	10.48
11	8	50	0.6500	11.11
8	9	50	0.8450	12.7
7	10	40	0.8450	16.6
10	11	40	0.8450	16.8
4	12	40	0.7800	12.9
14	13	60	0.7800	11.03
9	14	60	0.8450	11.25
1	15	40	0.6500	10.69

Table 4.12 shows the solubility data for the VW/n-heptane cloud point pressure design. In this case, the values were pre-chosen before the experimental work, and no fitting of raw data within excel was required to pursue the DOE analysis.

Table 4.12. Quantities of VW/n-heptane dissolved in scCO₂ and cloud point pressures for design.

Temperature (°C)	VW/n-heptane solution (mL)	Response: Pressure (MPa)
40	0.6500	10.69
40	0.7800	12.90
40	0.8450	16.60
40	0.8450	16.80
50	0.6500	10.48
50	0.6500	11.11
50	0.7800	11.84
50	0.7800	12.34
50	0.8450	12.70
60	0.6500	10.86
60	0.6500	10.27
60	0.7800	11.10
60	0.7800	11.03
60	0.8450	11.25
60	0.8450	11.85

According to the half-Normal Plot (Fig 4.19) A, B, and their interaction are significant factors in this design.

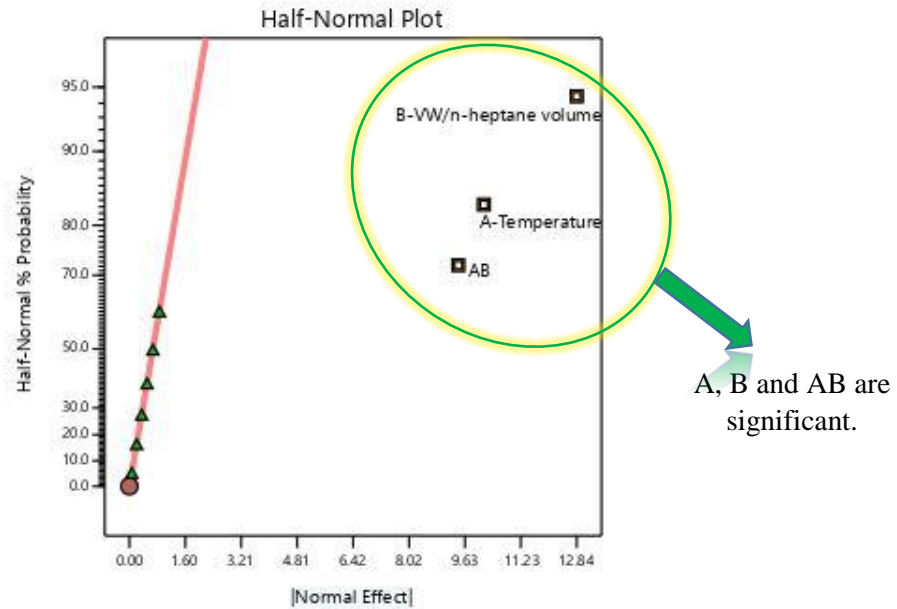


Figure 4.19. Half-Normal Plot from Design-Expert for VW/n-heptane solution in scCO₂.

The next step is to look at *ANOVA Table* (Table 4.13) from Design-Expert which provides information about the model, factors A, B, and their interaction. All the factors in the model are significant which is desirable.

Table 4.13. ANOVA table from design-expert for VW/n-heptane in scCO₂.

ANOVA for selected factorial model

Response 1: VW/n-heptane cloud point pressure

Source	Sum of Squares	df	Mean Square	F-value	p-value	
Model	56.17	8	7.02	60.18	< 0.0001	significant
A-Temperature	18.76	2	9.38	80.39	< 0.0001	
B-VW/n-heptane volume	18.52	2	9.26	79.37	< 0.0001	
AB	11.89	4	2.97	25.49	0.0007	
Pure Error	0.6999	6	0.1167			
Cor Total	56.87	14				

According to Normal Plot versus Residual and also Residual versus predicted in the **Diagnostics** part, everything is satisfactory and normality assumption is met.

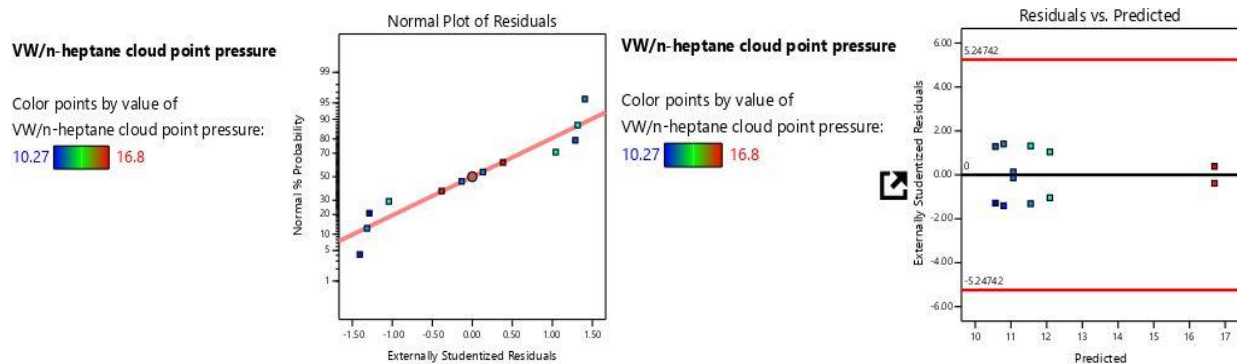


Figure 4.20. Normal plot of residual and residual versus predicted obtained from design-expert for VW/n-heptane in scCO₂.

At this point **Model graphs** extracted from Design-Expert provide complete information about all main factors, their interactions, and how they affect the cloud point pressure of VW/n-heptane solution in scCO₂.

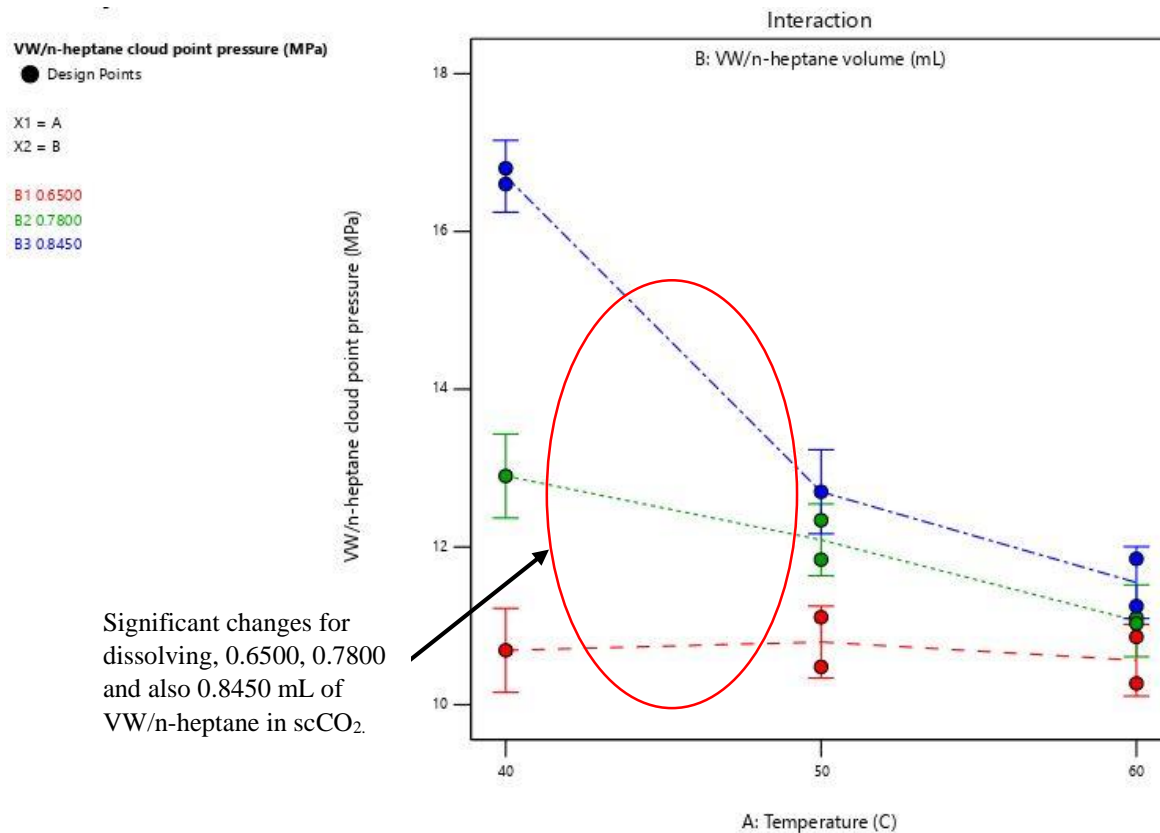


Figure 4.21. Interaction effect extracted from design-expert, for VW/n-heptane cloud point pressure (MPa) vs solution (mL).

As illustrated in Figure 4.21, one can see that at the lower temperature of 40 °C, higher pressure is needed to dissolve 0.8450 mL of VW/n-heptane solution in scCO₂. But, for the higher temperature lower pressure is required to dissolve the same amount of VW/n-heptane in scCO₂. For instance, at a lower temperature of T=40 °C, for dissolving 0.7800 and 0.8450 mL of VW/n-heptane in scCO₂ the cloud point pressure changes from 10.60 MPa to 16.80 MPa. This fact shows a significant change in the solubility of the VW/n-heptane in scCO₂ at different temperatures. Another important point is that for dissolving the lower amount of the hydrophobic solution in scCO₂ which is 0.6500 mL, the cloud point pressures at T = 40, 50, and 60 °C, are almost in the same range. Moreover, Design-Expert provides information for the interaction between factor A

(temperature) and factor B (VW/n-heptane solution) and also how they influence the cloud point pressure at different levels for all three temperatures in a 3D surface plot (4.22).

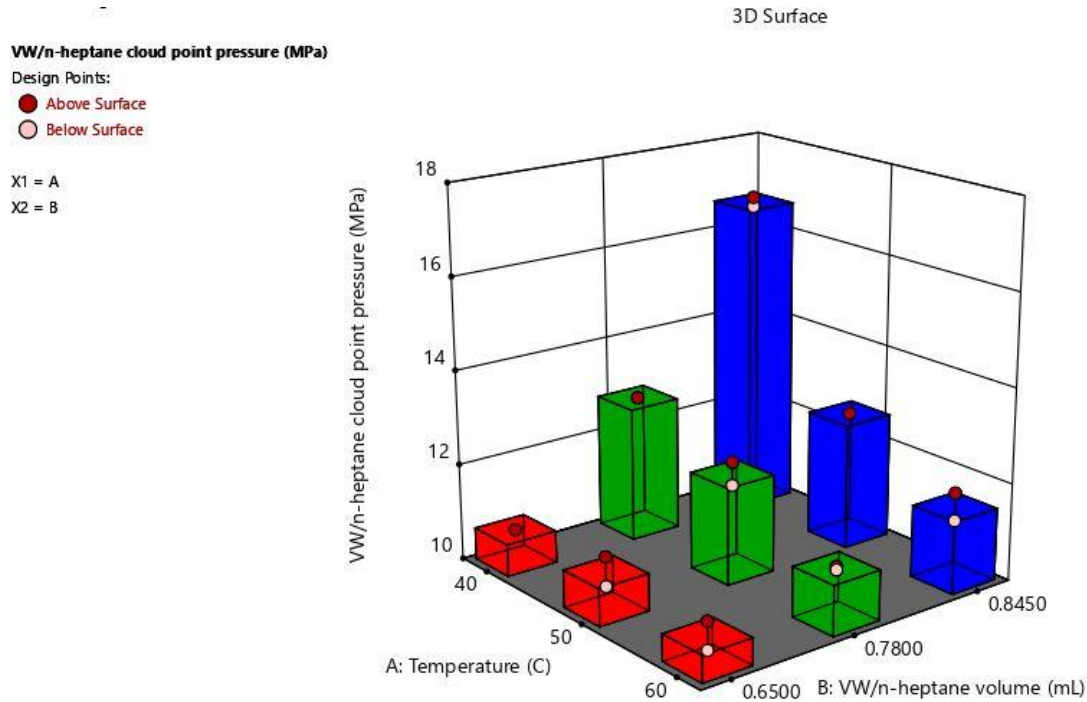


Figure 4.22. 3D surface plot from design-expert for VW/n-heptane cloud point pressure (MPa) VS temperature and amount of VW/n-heptane (mL).

The 3D surface plot exhibits the fact that higher solubilities of VW/n-heptane, 0.8450 (mL) is dissolved in scCO₂ at a lower pressure for T = 60 °C. Thus, at lower cloud point pressure, there is a maximum solubility of WV/n-heptane in scCO₂ for the higher temperature. This fact is clearly shown for 0.7800 and 0.8450 mL of VW/n-heptane in scCO₂ and for both these amounts lower pressures are needed at T = 60 °C to be dissolved in scCO₂. In addition, at the lower solubility of 0.6500 mL of VW/n-heptane solution, for all three temperatures, the cloud point pressures are close to each other and the cloud point pressure is between 10.27 and 11.11 MPa.

Furthermore, all these predicted results are valuable initial steps for conducting more cloud point experiments to observe and capture the changes of the solubility with respect to pressure at higher temperatures and finding the maximum solubility at higher pressures and temperatures not only for AKD/n-heptane and VW/n-heptane solutions in scCO₂ but also for other hydrophobic solutions with different cosolvents in scCO₂.

CHAPTER V

CONCLUSION AND RECOMMENDATIONS

5.1 Conclusion

In this study, maximum solubility of hydrophobic solutions such as AKD/n-heptane and VW/n-heptane in scCO₂ were investigated at different pressures and temperatures through cloud point experiments and subsequent solubility conditions were applied in SCI of AKD/n-heptane into paper substrates. CA measurements of various impregnated samples recorded with a Biolin OneAttention CA analyzer were performed to determine the highest CA, indicating enhanced hydrophobicity of the paper substrates for potential use in food packaging industries. Finally, solubility trends for wax/n-heptane solutions in scCO₂ were obtained and confirmed by DOE. Key conclusions include:

- 1- ***Solubility Measurements:*** Solubility measurements by cloud point experiments showed that for both waxes, at higher pressures more wax/n-heptane solutions were dissolved in scCO₂ for all three temperatures. In general, more VW/n-heptane was dissolved in scCO₂ than AKD/n-heptane. Cloud point experiments showed the highest amount of AKD/n-heptane (0.36 mL) dissolved in scCO₂ occurred at T = 60 °C and P = 161.89 bar. For VW/n-heptane, the highest solubility in scCO₂ was observed at T = 50 °C and P = 146.86 bar where 1.105 mL of the hydrophobic solution dissolved in scCO₂. The density of scCO₂ at these maximum conditions was 693 (kg/m³) and 643 (kg/m³) respectively, meaning that the presence of VW/n-

heptane hydrophobic solution with higher concentration is more soluble in scCO₂ at higher pressures.

- 2- **CA measurements:** Considering results obtained for AKD/n-heptane solubility in scCO₂, two solubility conditions were chosen for the SCI process of AKD/n-heptane to develop hydrophobicity for paper substrates (low and high P at each T investigated). The CA measurements of paper samples impregnated at T = 60 °C and 125.83 bar provided more hydrophobicity through the paper substrates with the CA of 130.71 °. Also, for the treated paper samples with different annealing temperatures, CA results demonstrated that immediate improvement in hydrophobicity is achieved by the impregnated sample at 60 °C and 148.10 bar with CA of 122.98 ° for annealing temperature of 160 °C for 4h. For samples annealed at T = 140 and 180 °C, there are peaks and troughs from day 0 to day 14. This was especially prevalent for impregnated samples at T = 40 °C with both pressures and all annealing temperatures investigated. For the impregnated paper at T = 50 °C and 156.10 bar, with an annealing temperature of 140 °C, the highest measured CA was 69.65 ° at Day 14.
- 3- **SEM Analysis:** SEM micrographs revealed the development of a more uniform surface without annealing treatment for the paper sample prepared at T = 40 °C and P=155.82 bar, while the more uniform distribution of AKD wax, and better micro-roughness through the matrix of the paper substrate was observed after annealing (4h, 160 °C) for samples prepared at T = 50 °C and P=156.10 bar. Therefore, choosing the most appropriate condition for SCI of AKD into paper substrates is essential for developing hydrophobicity for paper substrates.
- 4- **DOE:** DOE successfully identified trends in cloud point pressures for wax/n-heptane solutions in scCO₂. “Multilevel Categorical Design” showed that for both hydrophobic solutions (AKD/n-heptane and VW/n-heptane), higher amounts of wax/n-heptane are dissolved in

scCO₂ at higher pressures for all three temperatures, in agreement with the experimental data reported in the first conclusion. For AKD/n-heptane at T = 40 °C, much higher cloud point pressures are required to dissolve different amounts of AKD/n-heptane in scCO₂ compared with higher temperatures of 50 and 60 °C. For VW/n-heptane solutions, DOE demonstrated that for dissolving 0.845 mL of VW/n-heptane in scCO₂, a high cloud point pressure of 16.80 MPa was needed at T = 40 °C. But, for dissolving 0.65 mL of VW/n-heptane in scCO₂ the required cloud point pressure is almost the same for all three temperatures. Therefore, the significant difference in the required cloud point pressure to dissolve a specific amount of VW/n-heptane in scCO₂ is more evident for higher volumes of VW/n-heptane solutions.

5.2 Recommendations

At this point, the maximum solubility of VW/n-heptane in scCO₂ has been measured for different pressures and temperatures of 40, 50, and 60 °C. It is interesting to know whether applying these conditions for SCI can create better hydrophobicity for paper substrates comparing to AKD/n-heptane wax in scCO₂ or not. Since the *concentration of VW in heptane* is higher than AKD in n-heptane, it is highly likely to achieve higher CAs for the impregnated paper more readily using the solubility conditions compared with AKD/n-heptane. Also, consideration of annealing treatments at different temperatures will be useful to study with this wax, to see whether or not similar trends as those discovered with AKD are observed.

Furthermore, more food-grade waxes are appropriate for food packaging applications such as beeswax and carnauba wax. Performing cloud point solubility measurements in the same manner as that conducted with AKD and VW makes it easier for a researcher to not only find the optimum condition for SCI processes but also choose the most optimal wax. Another key fact that

may affect the results is choosing a cosolvent other than heptane and dissolving waxes with various concentrations in that cosolvent instead. Hexane may be a possible contender, and the solubility of different cosolvents with waxes in scCO₂ could be studied for future SCI and CA measurements.

Given the importance of the impregnation process to introduce hydrophobic substances into paper substrates, investigation of the interfacial interactions between the waxes and cellulose fibers may be studied using a quartz crystal microbalance (QCM-D). These studies may focus on the types of interfacial bonds formed between the wax deposits and the cellulose, as well as determine the kinetic rate of adhesion of the waxes onto the cellulose fibers.

LIST OF REFERENCES

- [1] V. P. Romani, B. Olsen, M. P. Collares, J. R. Meireles Oliveira, C. Prentice, V. G. Martins. Cold plasma and carnauba wax as strategies to produce improved bi-layer films for sustainable food packaging, *Food Hydrocolloids* 108 (2020) 106087.
- [2] M. R. Kasaai, A. Moosavi, Treatment of Kraft paper with citrus wastes for food packaging applications: Water and oxygen barrier properties improvement, *Food Packaging and Shelf Life* 12 (2017) 59 – 65.
- [3] J. Yadav, M. Datta, V. S. Gour, Developing Hydrophobic Paper as a Packaging Material Using Epicuticular Wax: A Sustainable Approach, *BioResources* 9(3), 5066-5072.
- [4] B. Hutton-prager, K. Adenekan, M. Sypnewski, A. Smith, M. Meados, C. Calicdan, Hydrophobic development and mechanical properties of cellulose substrates supercritically impregnated with food-grade waxes, *Cellulose* (2021) 28:1633–1646.
- [5] A. Ashok, C. R. Rejeesh, R. Renjith, Biodegradable Polymers for Sustainable Packaging Applications: A Review, *IJBB* (2016) 1-11.
- [6] C. Quan, O. Werner, L. W, C. Turner. Generation of superhydrophobic paper surfaces by a rapidly expanding supercritical carbon dioxide–alkyl ketene dimer solution, *J. of Supercritical Fluids* 49 (2009) 117–124.
- [7] T. F, T. Wang, A review of recent development of sustainable waxes derived from vegetable oils. *Current Opinion in Food Science* 16 (2017) 7–14.

- [8] K. Adenekan, B. Hutton-Prager, Sticky hydrophobic behavior of cellulose substrates impregnated with alkyl ketene dimer (AKD) via sub- and supercritical carbon dioxide, *Colloid and Surfaces A* 560 (2019) 154-163.
- [9] J. Drelich, Guidelines to measurements of reproducible contact angles using a sessile-drop technique, *Surface Innovations* (2013) 1-7.
- [10] B. H. J. Lee, N. A. Patankar, Contact angle hysteresis on rough hydrophobic surfaces, *Colloids and Surfaces A: Physicochem. Eng. Aspects* 248 (2004) 101–104.
- [11] G. M. N. J. Shirtcliffe, M. I. Newton, Contact-Angle Hysteresis on Super-Hydrophobic Surfaces, *Langmuir* 20 (2004) 10146-10149.
- [12] S. A. Kulinich, M. Farzaneh, Effect of contact angle hysteresis on water droplet evaporation from super-hydrophobic surfaces, *Applied Surface Science* 255 (2009) 4056–4060.
- [13] F. Chang, S. Hong, Y. Sheng, H. Tsao, High contact angle hysteresis of superhydrophobic surfaces: Hydrophobic defects, *Appl. Phys. Lett.* 95 (2009) 064102.
- [14] J. M. Dobbs, J. M. Wong, K. P. Johnston, Nonpolar Co-Solvents for Solubility Enhancement in Supercritical Fluid Carbon Dioxide, *J. Chem. Eng. Data*, 31 (1986) 303-308.
- [15] G. H. Brunner, *Supercritical Fluids as Solvents and Reaction Media*, Elsevier Science & Technology Books (2004) 1-630.
- [16] E. Kiran, P. G. Debenedetti, C. J. Peters, *Supercritical Fluids: Fundamental and Applications*, Springer (2000) 1-601.

- [17] S. Keskin, D. Kayrak-Talay, U. Akman, O. Hortacsu, A review of ionic liquids towards supercritical fluid applications, *J. of Supercritical Fluids* 43 (2007) 150–180.
- [18] M. Perrut, *Supercritical Fluid Applications: Industrial Developments and Economic Issues*, *Ind. Eng. Chem. Res.* 39 (2000) 4531-4535.
- [19] B. Lu, D. Zhang, W. Sheng, Solubility enhancement in supercritical solvents, *Pure & Appl. Chem.*, 62 (1990) 2277-2285.
- [20] Q. Shi, L. Jing, C. Xiong, C. Liu, W. Qiao, Solubility of Nonionic Hydrocarbon Surfactants with Different Hydrophobic Tails in Supercritical CO₂, *J. Chem. Eng. Data* 60 (2015) 2469–2476.
- [21] J. R Dean, *Applications of Supercritical Fluids in Industrial Analysis*, Springer (1993) 1-237.
- [22] E. Kiran, J. F. Brennecke, *Supercritical Fluid Engineering Science: Fundamentals and Applications*, American Chemical Society (1991) 1-413.
- [23] S. Jagtap, C. Magdum, D. Jadge, R. Jagtap, Solubility Enhancement Technique: A Review, *J. Pharm. Sci. & Res.* 10 (2018) 2205-2211.
- [24] J. M. Dobbs, J. M Wong, R. J. Lahiere, K. P. Johnston, Modification of Supercritical Fluid Phase Behavior Using Polar Cosolvents, *Ind. Eng. Chem. Res.* 26 (1987) 56-65.
- [25] K. L. Bennett, S. M. Ekart, G. S. Gurdial, C. L. Liott, C. A. Eckert, Cosolvent Interactions in Supercritical Fluid Solutions, *AIChE Journal*, 39 (1993) 235-248.

- [26] S. Z. Godse, M. S. Patil, S. M. Kothavade, R. B. Saudagar, Techniques for solubility enhancement of Hydrophobic drugs: A Review, *Journal of Advanced Pharmacy Education & Research*, 3 (2013) 403-414.
- [27] W. Wu, J. Zhang, B. Han, J. Chen, Z. Liu, T. Jiang, J. He, W. Li, Solubility of room temperature ionic liquid in supercritical CO₂ with and without organic compounds, *The Royal Society of Chemistry* (2003)1412-1413.
- [28] G. Li, D. Zhou, Q. Xu, G. Qiao, J. Yin, Solubility of Ionic Liquid [Bmim]Ac in Supercritical CO₂ Containing Different Cosolvents, *J. Chem. Eng. Data*. 63 (2018) 1596–1602.
- [29] C. Cadena, J. L. Anthony, J. K Shah, T. I. Morrow, J. F. Brennecke, E. J. Maginn, Why Is CO₂ So Soluble in Imidazolium-Based Ionic Liquids. *J. Am. Chem. Soc.* 126 (2004) 5300–5308.
- [30] K. Adenekan, B. Hutton-Prager, Modeling the solubility of Alkyl Ketene Dimer in supercritical carbon dioxide: Peng-Robinson, group contribution methods, and effect of critical density on solubility predictions, *Fluid Phase Equilibria* 507 (2020) 112415.
- [31] N. R. Foster, G. S. Gurdial, J. S. Yun, K. K. Liong, K. D. Tilly, S. S. Ting, H. Singh, J. H. Lee, Significance of the Crossover Pressure in Solid-Supercritical Fluid Phase Equilibria, *Ind. Eng. Chem. Res.* 30 (1991) 1955-1964.
- [32] E. Sahle-Demessie, U. R. Phillai, S. Junsophonsri, K. L. Levien, Solubility of Organic Biocides in Supercritical CO₂ and CO₂ + Cosolvent Mixtures, *J. Chem. Eng. Data*. 48 (2003) 541-547.

- [33] T. Rutter, B. Hutton-Prager, Investigation of hydrophobic coatings on cellulose-fiber substrates with in-situ polymerization of silane/siloxane mixtures, *International Journal of Adhesion and Adhesives* 86 (2018) 13–21.
- [34] B. Duracovic, Design of Experiments Application, Concepts, Examples: State of the Art, *engineering and Natural Science*, 5 (2017) 421-439.
- [35] T. Rakic, I. Kasagic-Vujanovic, M. Jovanovic, B. Jancic-Stojanovic, D. Ivanovic. COMPARISON OF FULL FACTORIAL DESIGN, CENTRAL COMPOSITE DESIGN, AND BOX-BEHNKEN DESIGN IN CHROMATOGRAPHIC METHOD DEVELOPMENT FOR THE DETERMINATION OF FLUCONAZOLE AND ITS IMPURITIES, *Analytical Letters*, 47 (2014) 1334–1347.

LIST OF APENDIX

APENDIX A

Cloud Point Images for wax/n-heptane

a) Before pressurization – 0.2325 mL
AKD/n-heptane inside the cell.



b) Cloud Point



Figure A.1 Cloud point observed at $T=40\text{ }^{\circ}\text{C}$ and $P=165.47\text{ bar}$.

c) Before pressurization - 0.0525
mL AKD/n-Hep inside the cell.



d) Cloud Point



Figure A.2 Cloud point observed at $T=50\text{ }^{\circ}\text{C}$ and $P=110.32\text{ bar}$.

e) Before pressurization - 0.0525 mL AKD-Hep inside the cell.



f) Cloud Point



Figure A.3 Cloud point observed at $T=60.3\text{ }^{\circ}\text{C}$ and $P=106.87\text{ bar}$.

g) Before pressurization - 0.3600 mL AKD-Hep inside the cell.



h) Cloud Point



Figure A.4 Cloud point observed at $T=57.4\text{ }^{\circ}\text{C}$ and $P=161.89\text{ bar}$.

i) Before pressurization – 0.65 mL VW/Hep inside the cell.



j) Cloud Point



Figure A.5 Cloud point observed at $T=40.3\text{ }^{\circ}\text{C}$ and $P=106.87\text{ bar}$.

k) Before pressurization – 0.78 mL VW-Hep inside the cell.

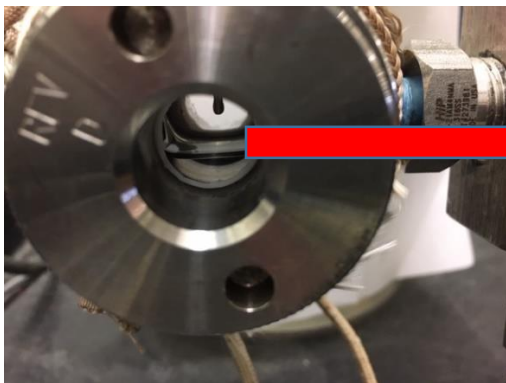


l) Cloud Point



Figure A.6 Cloud point observed at $T=41.7\text{ }^{\circ}\text{C}$ and $P=166.03\text{ bar}$.

k) Before pressurization – 1.105 mL VW/Hep inside the cell.



l) Cloud Point



Figure A.7 Cloud point observed at $T=49.7\text{ }^{\circ}\text{C}$ and $P=146.86\text{ bar}$.

VITAE

Arghavan Beheshtimaal

Education

July 2021 **MS Chemical Engineering** | University of Mississippi | GPA: 3.33/4.00.

May 2015 **MS Chemical Engineering** | Azad University, Iran | GPA: 3.35/4.00.

Feb 2010 **BS Chemical Engineering** | Azad University, Iran | GPA: 3.71/4.00.

Experiences

Graduate Research & Teaching Assistant | University of Mississippi, Oxford

Solubility Measurements of Hydrophobic Solutes in Supercritical Carbon Dioxide and Subsequent Impregnation into Paper Substrates for Surface Modifications:

- Measured solubility limits to find optimum pressures & temperatures for paper impregnation process.
- Successfully modified paper surface in scCO₂ to create hydrophobicity against moisture.
- Carried out Contact Angle (CA) measurements to find the highest CAs at different conditions.
- Design of Experiment (DOE) for solubility data to predict cloud point pressures and carry out statistical analysis.

Mar 2014-Dec 2017 **Research Project** | Azad University, Iran

Modeling and Simulating Gas Hydrate Formation in the Presence of Promoter:

- Predicted single gas hydrates formation conditions by MATLAB to evaluate the applied model.
- Developed Thermodynamic Model by MATLAB program to enhance gas hydrate formation pressure.
- Applied Genetic Algorithm (GA) to optimize single and mixed gas hydrates formation.
- Achieved optimum gas hydrate formation pressure by NRTL & UNIFAC Models for single and mixed gas hydrates.

Sep 2009-Feb 2010 **Final Project Undergrad** | Azad University, Iran

Project Title: Equipment design, Layout and economic estimation for producing engine oils in plants, licensed under Licomoly.

Jun 2009-Sep 2009 **Chemical Engineering Intern** | NARGAN Engineers & Constructors | Iran

- Attended process sector of NARGAN Engineers to learn and prepare Data sheet, PFD, P&ID, etc.
- Improved my process simulation skills with HYSYS, HTRI and Aspen-Bjac software and subsequently earn their Certificates.

Publication(s)

1. Beheshtimaal, A; Hutton-Prager B. Solubility Measurements of Wax/n-heptane in Supercritical Carbon Dioxide by Cloud Point Experiment for Surface Improvement. Fluid Phase Equilibria (In progress-2021).

2. Beheshtimaal, A.; Haghtalab, A. Thermodynamic modeling of hydrate formation conditions using different activity coefficient models in the presence of tetrahydrofuran (THF). Chemical Engineering Research and Design. 2018, 129, 150-159.

Conference

Beheshtimaal, A and Hutton-Prager, B (2021). “Solubility Measurements of AKD-heptane in Supercritical CO₂ by Cloud Point Experiment for Surface Improvement in Impregnation Processes.” Novel Materials, 048_Session 11. 18th European Meeting on Supercritical Fluids (virtual), May 4 – 6, France.

Award(s)

Summer Graduate Research Assistantship Recipient (2021).

Certificates

1-In-progress: Six Sigma Yellow Belt offered by University System of Georgia - Coursera

2-Machine Learning for all issued by Coursera.

3-Diploma De La Lengua Española from Iran Language Institute.

4-Matlab issued by “Falat Ghareh Development & Industry”.

5-Hysys earned from “Falat Ghareh Development & Industry”.

6-Aspen-Bjac & HTRI earned from “Novin Parsian Institute of sciences”.

7-Certificate of Completion in English from Safir Language Academy